

Supporting information for

Symmetry-Breaking in Self-Assembled M_4L_6 Cage Complexes

Wenjing Meng, Tanya K. Ronson, and Jonathan R. Nitschke*

Department of Chemistry, University of Cambridge, Lensfield Road, Cambridge, 1EW, UK

*E-mail: jrn34@cam.ac.uk

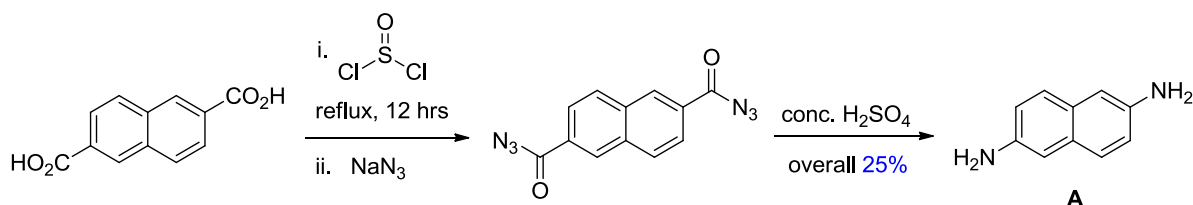
Table of Contents

General experimental procedures.....	S1
1. Synthesis and characterization of ligand subcomponents.....	S1
2. Characterization of complexes.....	S4
3. Metal displacement.....	S36
4. Discussion of symmetry breaking.....	S37
References.....	S38

General experimental procedures

All manipulations were carried out using reagents of the highest commercially available purity. ^1H NMR spectra were recorded at 400 MHz or 500 MHz. ^{13}C NMR, COSY, HMQC (Heteronuclear Multiple Quantum Correlation) and DOSY (Diffusion Ordered Spectroscopy) spectra were recorded on a 500 MHz spectrometer. NMR spectra were referenced to the residual ^1H or ^{13}C NMR signal of the solvent and were recorded at 298 K unless otherwise specified. The ^1H NMR spectra of **1a**, **1b**, **1c** and **3a** were assigned with the help of COSY and HMQC measurements. Mass spectra were recorded using electrospray ionisation mass spectrometry (ESI-MS) in acetonitrile.

1. Synthesis and characterization of ligand subcomponents



Scheme S1: Synthetic pathway for diamine **A** (S1).

Naphthalene-2,6-dicarboxylic acid (0.55 g, 2.54 mmol, 1 equiv.) was mixed with SOCl_2 (5 mL). The resulting mixture was refluxed under N_2 for 20 hours. The solvent was removed under high vacuum and the residue was dissolved in distilled acetone (100 mL). To this acetone solution was added an aqueous solution (12.5 mL) of NaN_3 (1.29 g, 19.8 mmol, 7.8 equiv.) at 0°C . After the addition the ice bath was removed and the mixture was stirred at room temperature for 2 hours. White solid precipitated out. It was collected by filtration and washed with water to give the desired product naphthalene-2,6-dicarbonylazide which was used in the next step without further purification.

The crude naphthalene-2,6-dicarbonylazide was added portion-wise into concentrated H_2SO_4 (30 mL) at 0°C . After addition the reaction mixture was stirred at room temperature for 2 hours and slowly poured onto ice (30 mL). The resulting solution was made alkaline by the addition of a 50% aqueous solution of NaOH . The organics were extracted with EtOAc , washed with brine, dried (MgSO_4) and evaporated to dryness to afford the desired product naphthalene-2,6-diamine **A** as light brown solid (100 mg, 25% overall).

^1H NMR (DMSO, 400 MHz): 7.24 (2H, d, J 8.60, 4-naphthalene), 6.77 (2H, dd, J 8.60, 1.80, 3-naphthalene), 6.68 (2H, s, 1-naphthalene), 4.82 (4H, br, NH_2); ^{13}C $\{^1\text{H}\}$ NMR (125 MHz, CDCl_3):

141.56, 129.40, 127.23, 119.06, 109.55; ESI-MS $[M+H]^+$ 159.0917; Found: C, 73.80; H, 6.29; N, 16.40 %. Calc. for $C_{10}H_{10}N_2 \cdot 0.25H_2O$: C, 73.82; H, 6.50; N, 17.22 %.

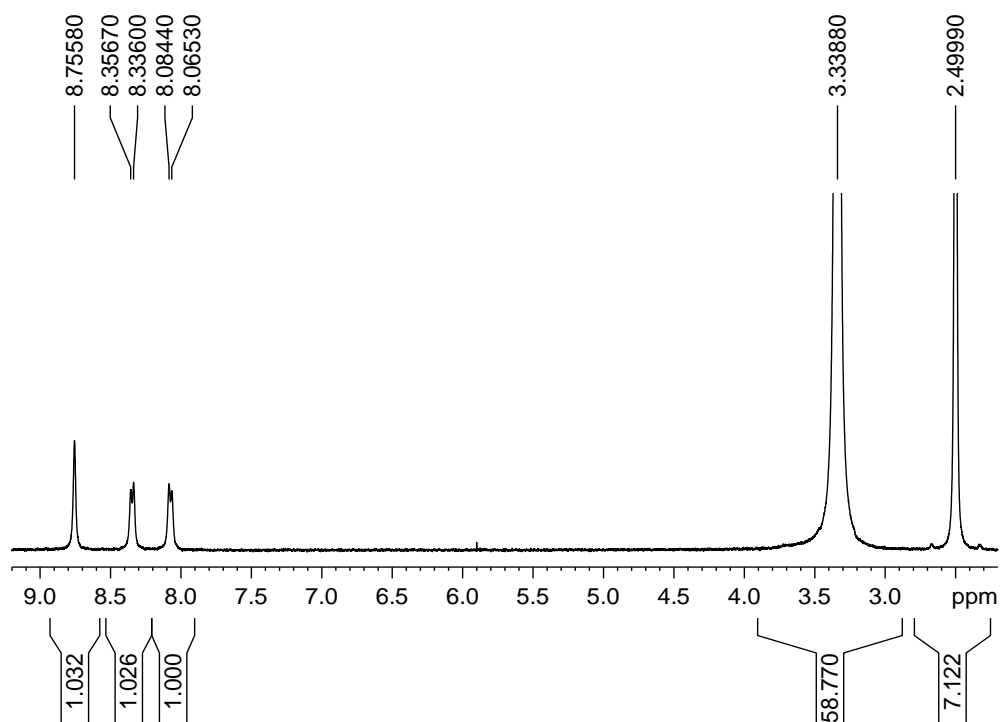


Figure S1. 1H NMR spectrum for naphthalene-2,6-dicarbonylazide.

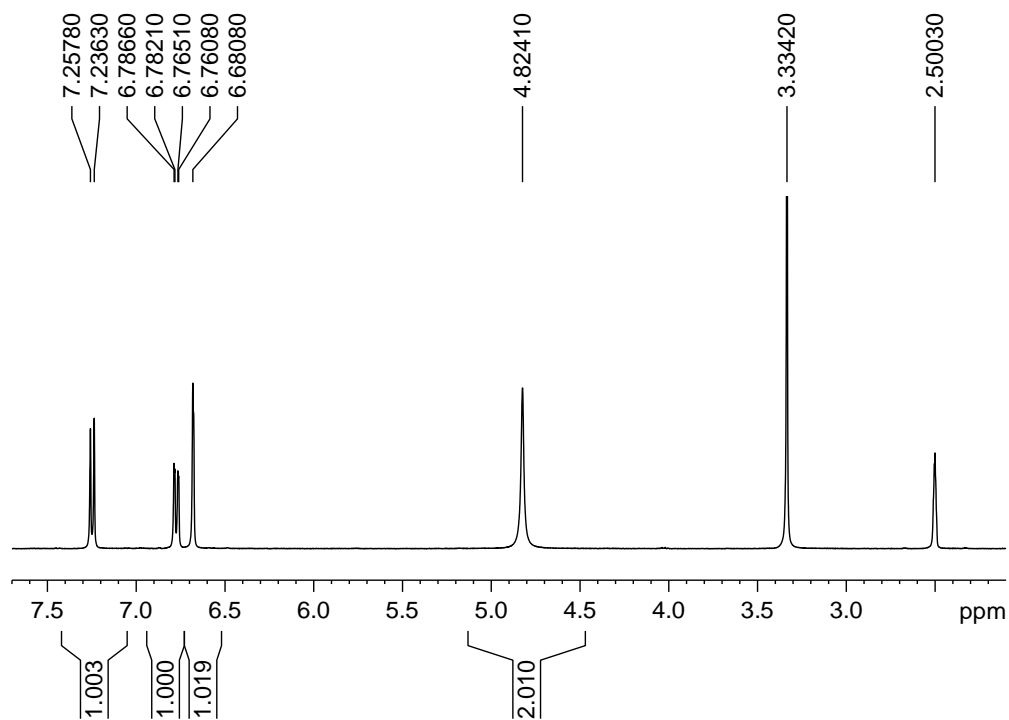


Figure S2. 1H NMR spectrum for A.

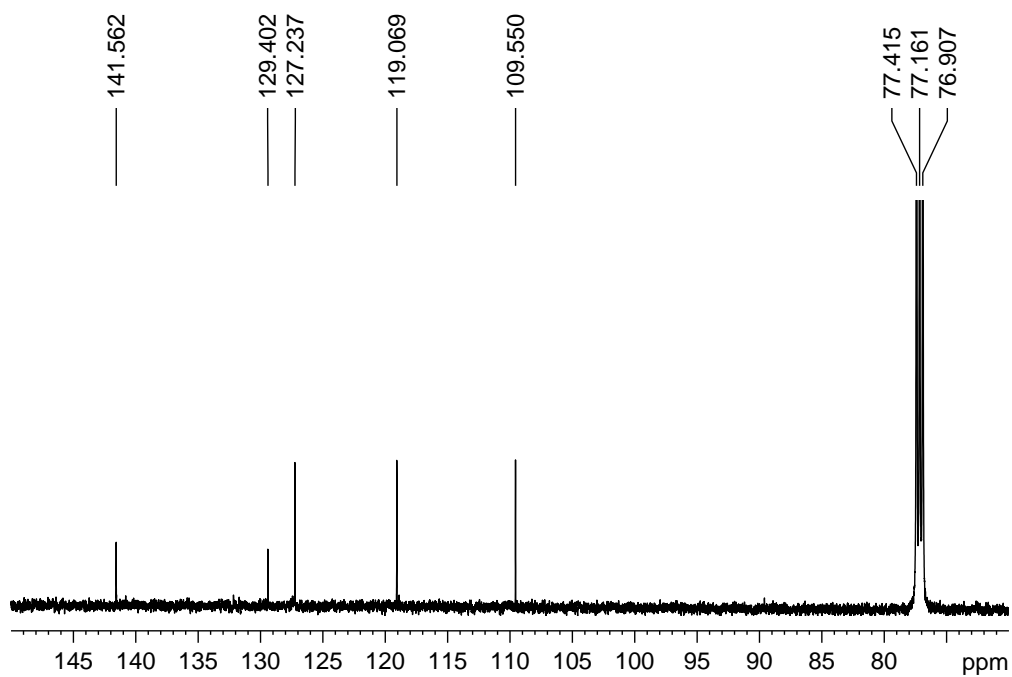
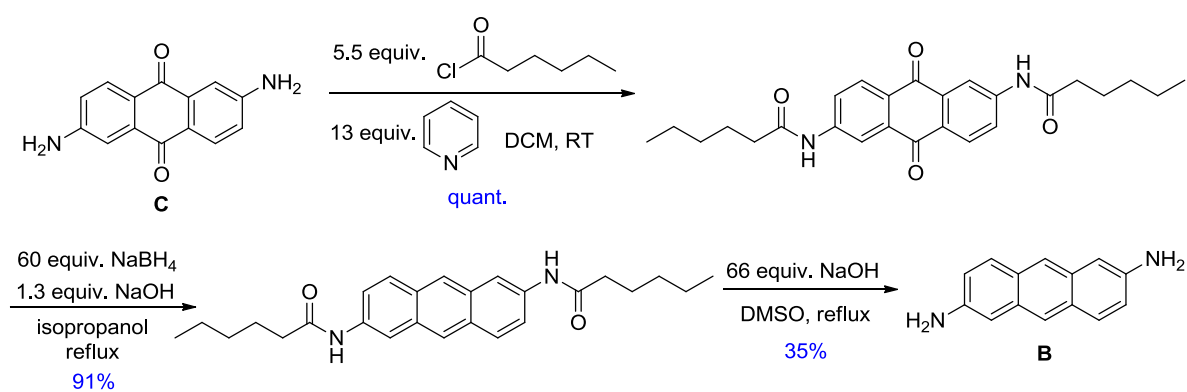


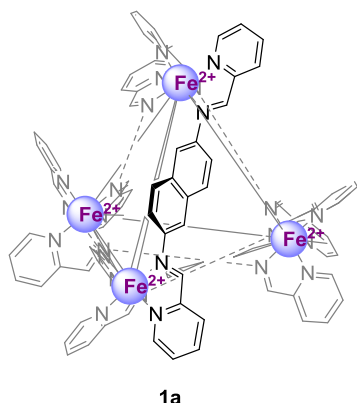
Figure S3. ^{13}C NMR spectrum for **A**.

Anthracene-2,6-diamine **B** was synthesized following a literature procedure (S2):



Scheme S2: Synthetic pathway for anthracene-2,6-diamine **B**.

2. Characterization of complexes



Synthesis of 1a·ClO₄. A (5.0 mg, 31.6 μmol, 3 equiv.), 2-pyridinecarboxaldehyde (6.0 μL, 63.2 μmol, 6 equiv.) and Fe(ClO₄)₂ (5.4 mg, 21.1 μmol, 2 equiv.) were mixed in MeCN (5 mL). The resulting solution was heated at 50°C for 12 hrs. Diethyl ether was added to precipitate the solid. The mixture was centrifuged and the solvent was decanted. The solid was dried and high vacuum to give the desired product **1a**·ClO₄ as dark purple solid (8.7 mg, 54%). ¹H NMR (CD₃CN, 400 MHz): 9.84 (2H, s imine-*H*), 9.59 (1H, s imine-*H*), 9.32 (1H, s imine-*H*), 9.28 (1H, s imine-*H*), 9.24-9.23 (2H, Ar-*H*), 9.18-9.09 (3H, Ar-*H*), 8.90-8.87 (3H, Ar-*H*), 8.75-8.71 (4H, Ar-*H*), 8.50-8.30 (21H, Ar-*H*), 7.60-8.13 (22H, Ar-*H*), 7.37-7.48 (8H, Ar-*H*), 6.87-6.83 (2H, Ar-*H*), 6.61 (1H, d, *J* 8.44, Ar-*H*), 6.50 (1H, s, Ar-*H*), 6.41 (1H, d, *J* 8.12, Ar-*H*), 6.37-6.32 (2H, Ar-*H*), 6.19-6.28 (4H, Ar-*H*), 6.09 (1H, d, *J* 9.52, Ar-*H*), 6.00-5.77 (7H, Ar-*H*), 5.61 (1H, s, Ar-*H*), 5.36 (1H, d, *J* 8.24, Ar-*H*), 5.33 (1H, s, Ar-*H*), 5.16-5.13 (2H, Ar-*H*), 4.86 (1H, s, Ar-*H*), 4.50 (1H, d, *J* 6.92, Ar-*H*), 4.36 (1H, s, Ar-*H*), 4.23 (1H, d, *J* 9.16, Ar-*H*), 4.08 (1H, s, Ar-*H*); ¹³C {¹H} NMR (125 MHz, CD₃CN): 178.78, 178.31, 177.50, 177.42, 177.13, 176.81, 176.47, 176.06, 175.70, 175.65, 175.08, 173.78, 159.15, 159.06, 159.01, 158.96, 158.68, 158.62, 158.40, 158.07, 157.70, 157.57, 157.54, 157.35, 157.01, 156.85, 156.83, 156.74, 156.47, 156.43, 156.42, 156.24, 151.32, 150.91, 150.77, 150.75, 150.50, 150.26, 150.16, 150.12, 149.66, 149.62, 149.48, 141.13, 141.00, 140.91, 140.74, 140.70, 140.61, 140.50, 134.27, 133.66, 133.59, 133.36, 132.99, 132.97, 132.91, 132.85, 132.76, 132.66, 132.63, 132.49, 132.31, 132.20, 132.15, 132.04, 132.00, 131.93, 131.83, 131.81, 131.78, 131.70, 131.60, 131.57, 131.52, 131.50, 131.42, 131.36, 131.28, 130.94, 130.81, 130.72, 130.60, 130.03, 129.89, 128.89, 124.47, 123.56, 123.50, 123.24, 123.10, 122.98, 122.83, 122.72, 122.70, 122.57, 122.37, 122.21, 122.11, 121.93, 121.53, 121.02, 120.78, 120.62, 120.35, 120.09, 120.04, 119.92, 119.80; ESI-MS: [**1a**(ClO₄)₄]⁴⁺ 659.74, [**1a**(ClO₄)₅]³⁺ 912.65, [**1a**(ClO₄)₆]²⁺ 1419.21. Found: C, 52.48; H, 3.41; N, 11.00 %. Calc. for C₁₃₂H₉₆Cl₈Fe₄N₂₄O₃₂: C, 52.20; H, 3.19; N, 11.07 %.

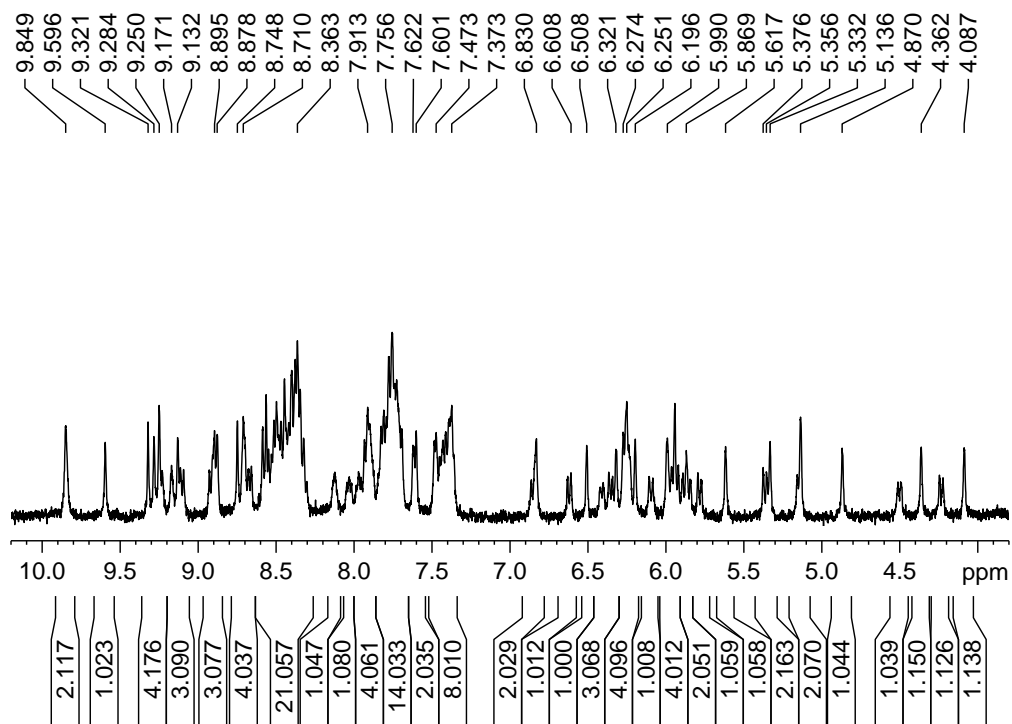


Figure S4a. ^1H NMR spectrum for $\mathbf{1a}\cdot\text{ClO}_4$ (in CD_3CN).

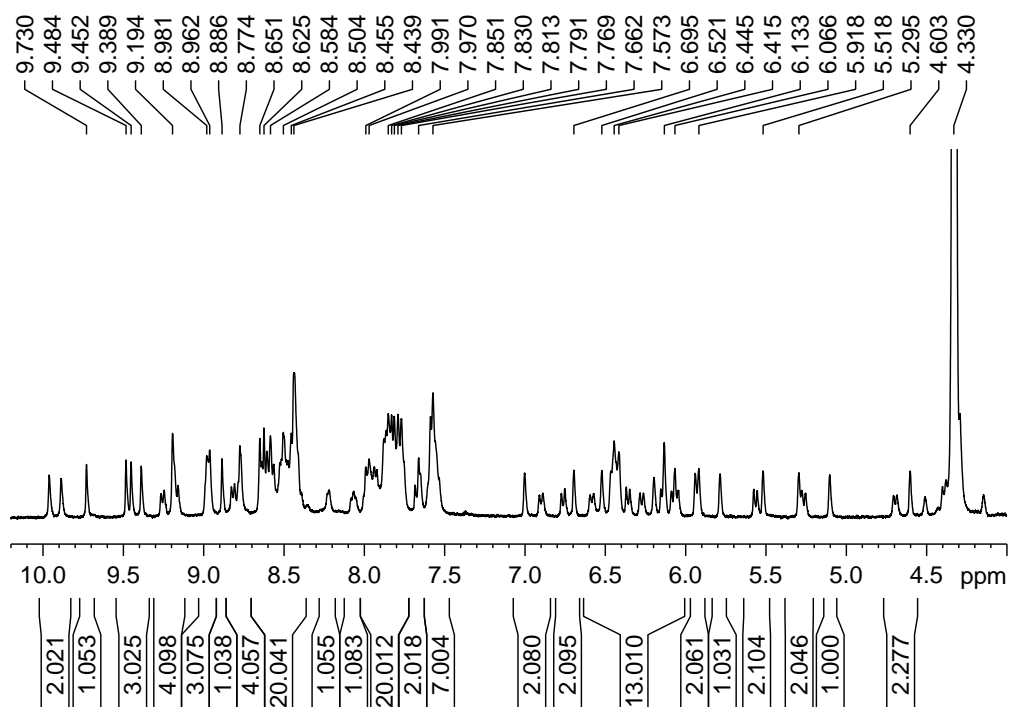


Figure S4b. ^1H NMR spectrum for $\mathbf{1a}\cdot\text{ClO}_4$ (in CD_3NO_2).

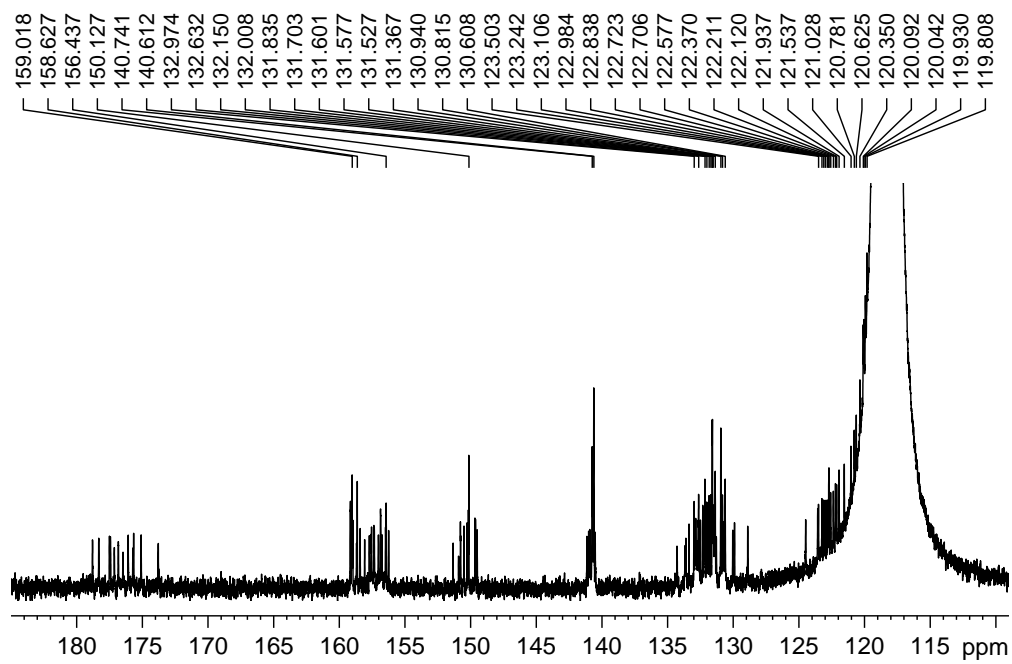


Figure S5. ^{13}C NMR spectrum for **1a**·ClO₄ (in CD₃CN).

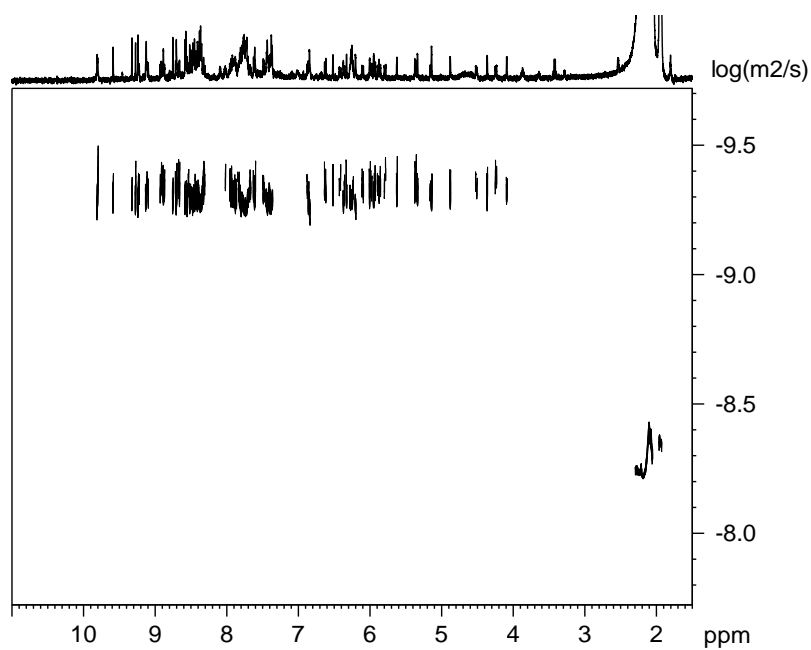


Figure S6. DOSY spectrum (in CD₃CN) for **1a**·ClO₄. $r_{\text{H}} = 12 \text{ \AA}$.

Synthesis of $\mathbf{1a}\cdot\text{OTf}$. **A** (5.0 mg, 31.6 μmol , 3 equiv.), 2-pyridinecarboxaldehyde (6.0 μL , 63.2 μmol , 6 equiv.) and $\text{Fe}(\text{OTf})_2$ (7.5 mg, 21.1 μmol , 2 equiv.) were mixed in MeCN (5 mL). The resulting solution was heated at 50°C for 12 hrs. Diethyl ether was added to precipitate the solid. The mixture was centrifuged and the solvent was decanted. The solid was dried and high vacuum to give the desired product $\mathbf{1a}\cdot\text{OTf}$ as dark purple solid (13.3 mg, 74%). ^1H NMR (CD_3CN , 500 MHz): 9.81 (1H, s, imine-*H*), 9.76 (1H, s, imine-*H*), 9.59 (1H, s, imine-*H*), 9.31 (1H, s, imine-*H*), 9.30 (1H, s, imine-*H*), 9.24 (1H, s, imine-*H*), 9.20 (1H, s, imine-*H*), 9.19 (1H, d, *J* 6.55, Ar-*H*), 9.11 (1H, d, *J* 7.95, Ar-*H*), 9.03 (1H, s, imine-*H*), 8.90-8.89 (2H, Ar-*H*), 8.87 (1H, Ar-*H*), 8.84 (1H, s, imine-*H*), 8.82-8.66 (2H, Ar-*H*), 8.68 (1H, s, imine-*H*), 8.65 (1H, s, imine-*H*), 8.56 (1H, s, imine-*H*), 8.55-8.29 (16H, Ar-*H*), 8.00-7.98 (2H, Ar-*H*), 7.92-7.68 (18H, Ar-*H*), 7.62-7.59 (3H, Ar-*H*), 7.47 (1H, d, *J* 5.20, Ar-*H*), 7.40-7.33 (8H, Ar-*H*), 6.85 (1H, d, *J* 8.90, Ar-*H*), 6.83 (1H, s, Ar-*H*), 6.57 (1H, d, *J* 8.60, Ar-*H*), 6.50 (1H, s, Ar-*H*), 6.42 (1H, d, *J* 8.60, Ar-*H*), 6.31-6.22 (5H, Ar-*H*), 6.18 (1H, s, Ar-*H*), 6.13 (1H, d, *J* 7.90, Ar-*H*), 6.03 (1H, s, Ar-*H*), 5.98-5.96 (2H, Ar-*H*), 5.93-5.89 (3H, Ar-*H*), 5.77 (1H, dd, *J* 8.70, 1.90, Ar-*H*), 5.60 (1H, s, Ar-*H*), 5.41 (1H, d, *J* 8.65, Ar-*H*), 5.31 (1H, s, Ar-*H*), 5.16 (1H, s, Ar-*H*), 5.13 (1H, d, *J* 8.55, Ar-*H*), 4.84 (1H, s, Ar-*H*), 4.49 (1H, d, *J* 9.25, Ar-*H*), 4.40 (1H, d, *J* 1.50, Ar-*H*), 4.22 (1H, dd, *J* 8.50, 1.40, Ar-*H*), 4.08 (1H, s, Ar-*H*); ^{13}C $\{^1\text{H}\}$ NMR (125 MHz, CD_3CN): 178.60, 177.56, 177.48, 177.36, 177.18, 177.02, 176.21, 176.03, 175.83, 175.22, 174.10, 159.23, 159.20, 159.19, 159.14, 159.08, 158.93, 158.79, 158.70, 158.57, 158.31, 157.83, 157.81, 157.67, 157.49, 157.40, 157.12, 157.02, 156.96, 156.84, 156.62, 156.55, 156.32, 151.43, 151.01, 150.79, 150.77, 150.42, 150.36, 150.26, 150.23, 149.93, 149.83, 149.61, 141.16, 141.07, 140.92, 140.88, 140.83, 140.73, 140.64, 134.33, 133.72, 133.46, 133.24, 133.08, 133.03, 132.98, 132.73, 132.60, 132.56, 132.40, 132.31, 132.29, 132.24, 132.09, 132.02, 131.97, 131.94, 131.87, 131.84, 131.79, 131.73, 131.72, 131.65, 131.61, 131.58, 131.47, 131.46, 131.36, 131.33, 131.09, 131.06, 131.03, 130.98, 130.94, 130.79, 130.77, 130.04, 130.01, 129.02; ESI-MS: $[\mathbf{1a}(\text{OTf})_4]^{4+}$ 709.49, $[\mathbf{1a}(\text{OTf})_5]^{3+}$ 995.69, $[\mathbf{1a}(\text{OTf})_6]^{2+}$ 1568.21. Found: C, 47.16; H, 2.79; N, 9.20 %. Calc. for $\text{C}_{140}\text{H}_{96}\text{F}_{24}\text{Fe}_4\text{N}_{24}\text{O}_{24}\text{S}_8\cdot 7\text{H}_2\text{O}$: C, 47.23; H, 3.11; N, 9.44 %.

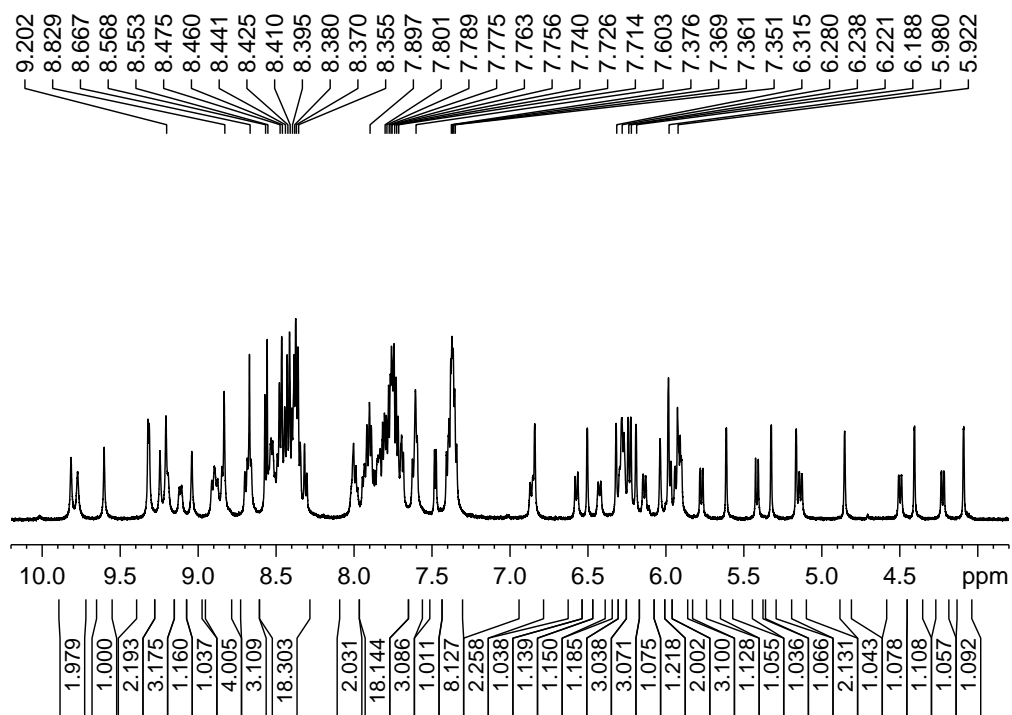


Figure S7. ^1H NMR spectrum for **1a**·OTf.

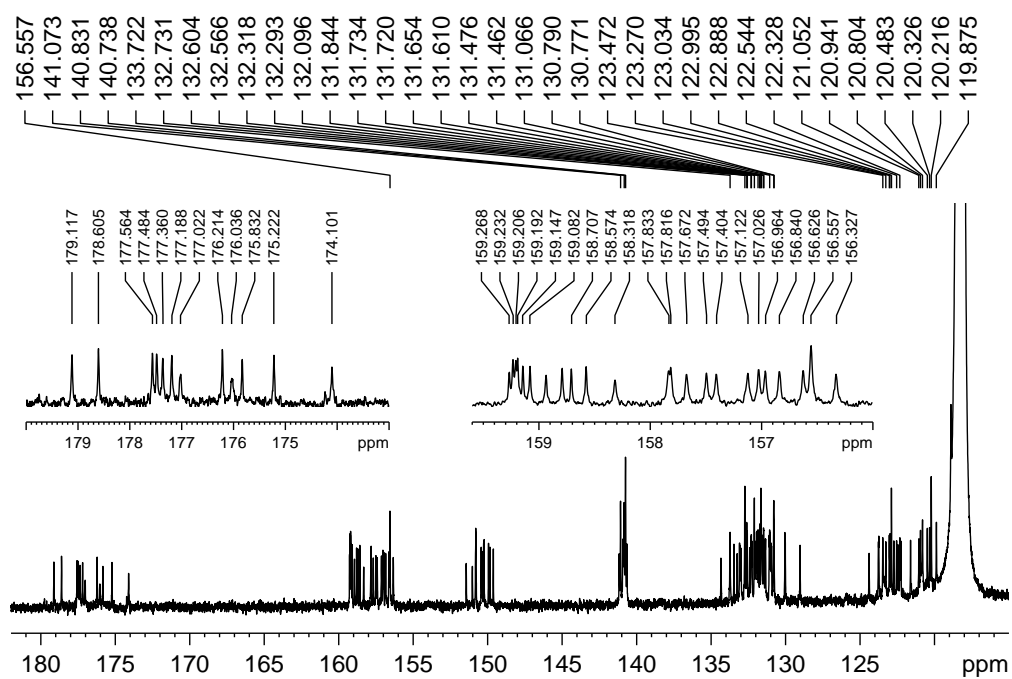


Figure S8. ^{13}C NMR spectrum for **1a**·OTf.

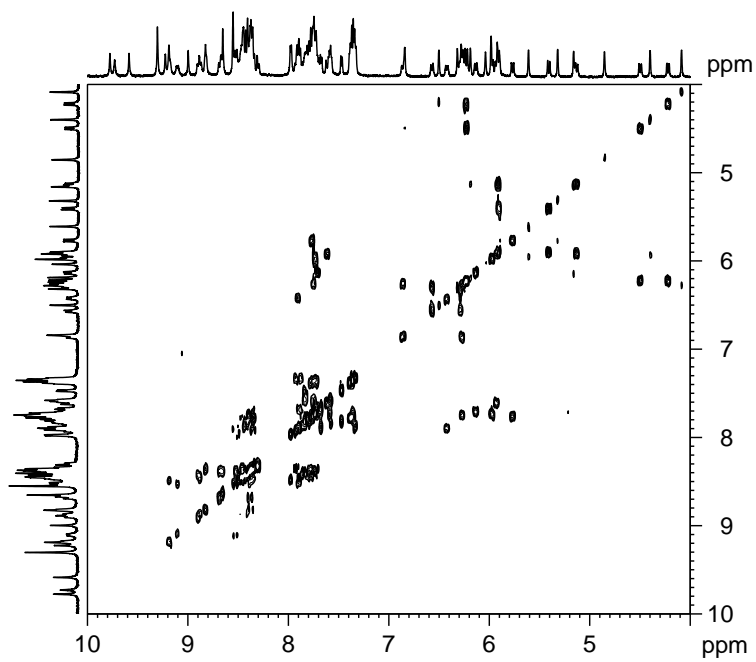


Figure S9. ^1H - ^1H COSY spectrum for **1a**·OTf.

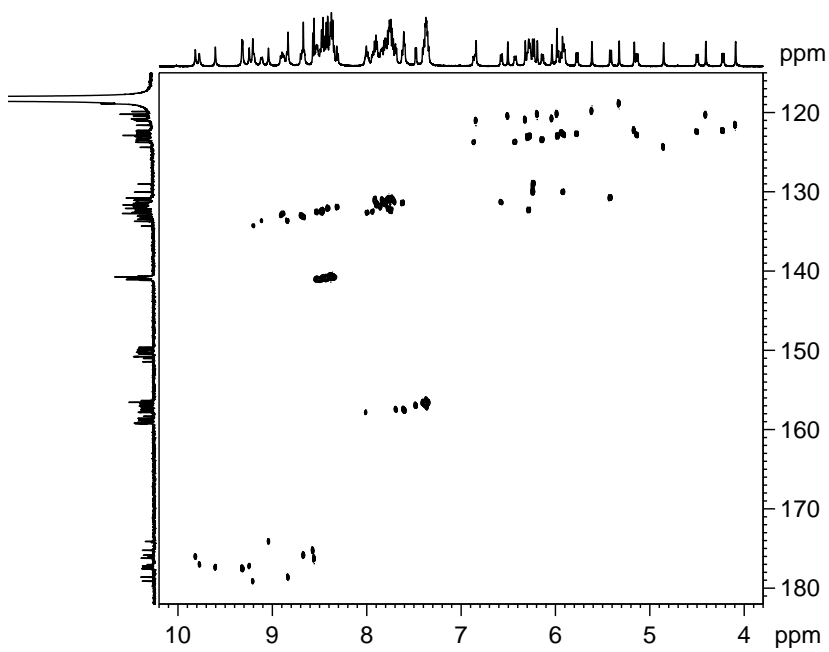


Figure S10a. HMQC spectrum for **1a**·OTf.

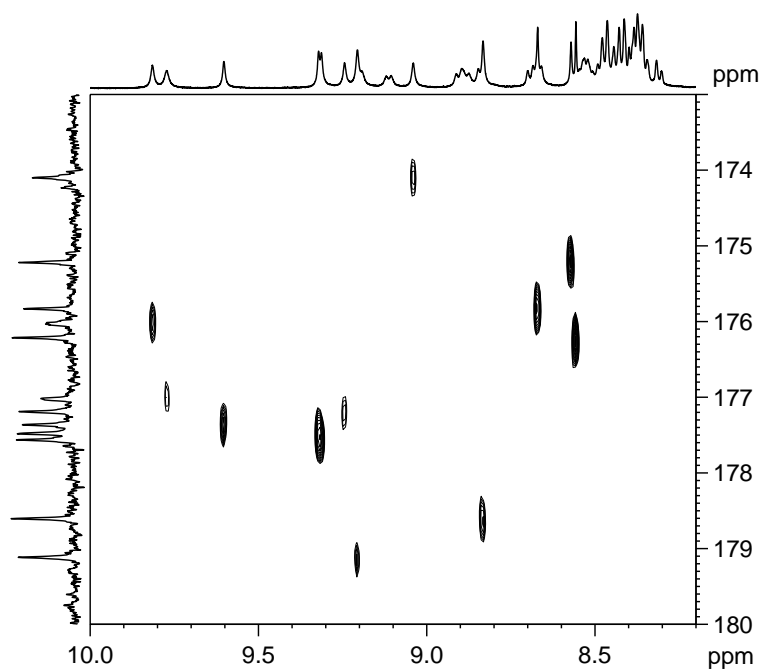


Figure S10b. HMQC spectrum for **1a**·OTf zoom of imine region.

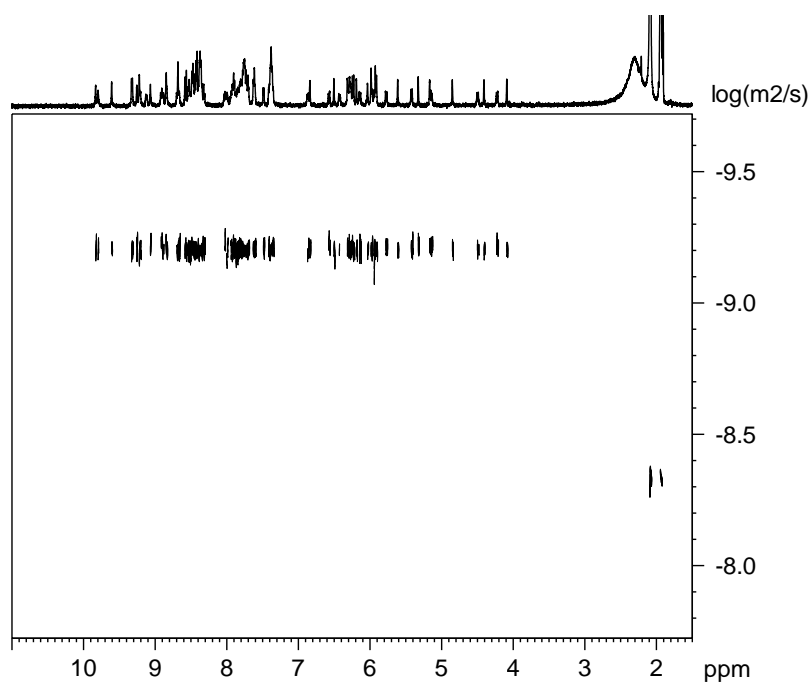


Figure S11. DOSY spectrum for **1a**·OTf. $r_{\text{H}} = 10.3 \text{ \AA}$.

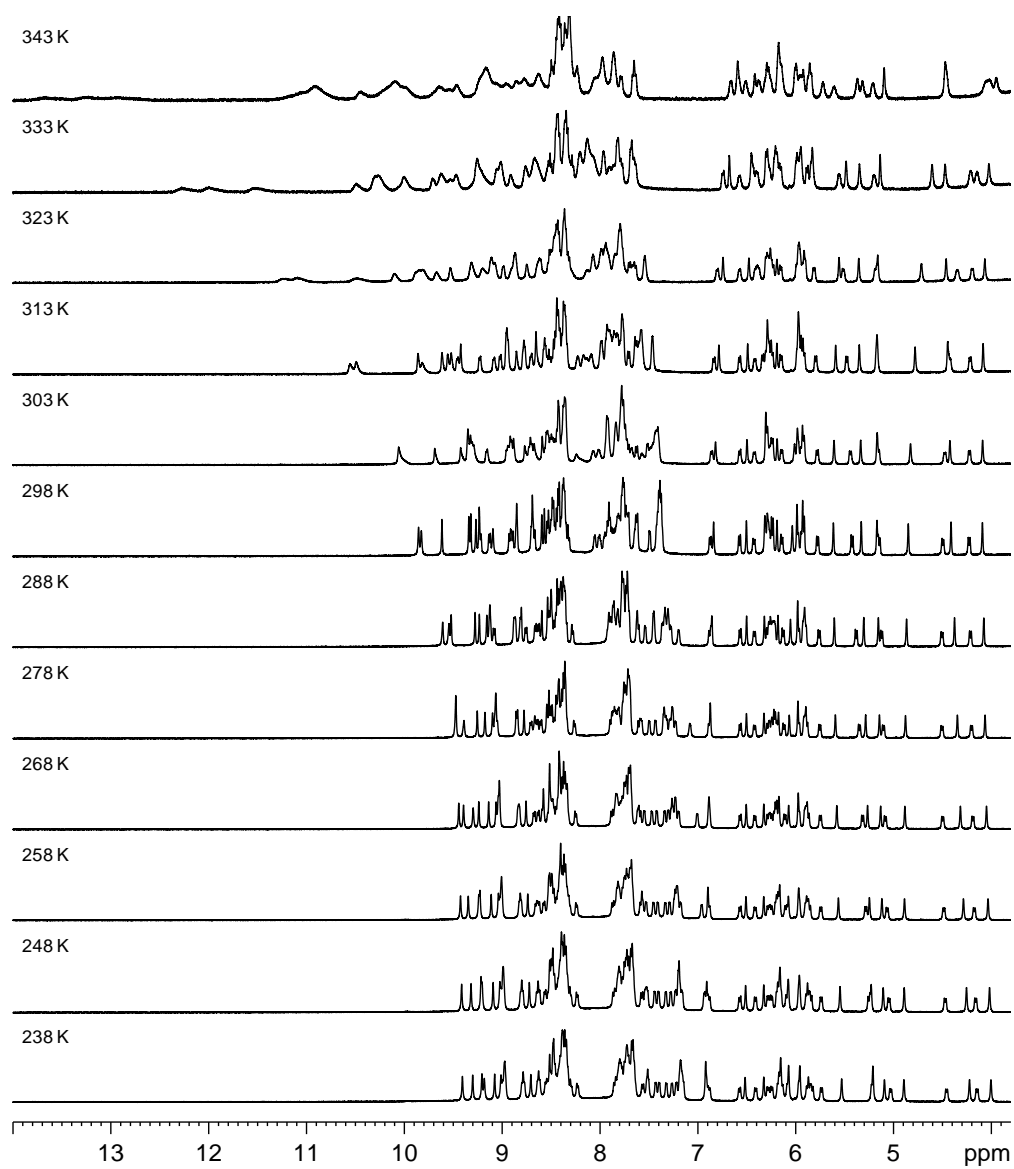
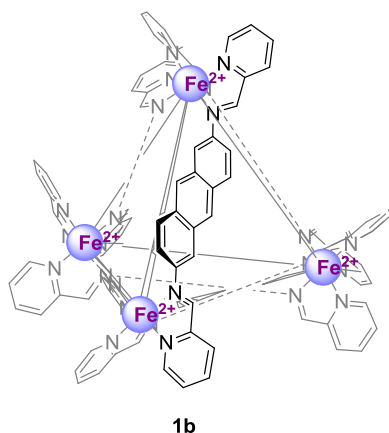


Figure S12. Variable temperature ^1H spectra for $1\mathbf{a}\cdot\text{OTf}$.



Synthesis of **1b·OTf. **B**** (20 mg, 96 μmol , 3 equiv.), 2-pyridinecarboxaldehyde (18.2 μL , 0.19 mmol, 6 equiv.) and $\text{Fe}(\text{OTf})_2$ (23 mg, 64 μmol , 2 equiv.) were mixed in MeCN (5 mL). The resulting solution was heated at 50°C for 12 hrs. Diethyl ether was added to precipitate the solid. The mixture was centrifuged and the solvent was decanted. The solid was dried and high vacuum to give the desired product **1b**·OTf as dark red solid (33 mg, 55%). ^1H NMR (CD_3CN , 500 MHz): 9.31 (1H, s, imine-*H*), 9.24 (1H, s, imine-*H*), 9.22 (1H, s, imine-*H*), 9.21 (1H, s, imine-*H*), 9.12 (1H, s, imine-*H*), 9.10 (1H, s, imine-*H*), 9.04 (1H, s, imine-*H*), 8.98 (1H, s, imine-*H*), 8.90-8.60 (11H, Ar-*H*), 8.50-8.34 (23H, Ar-*H*), 8.11-7.79 (23H, Ar-*H*), 7.82 (1H, d, J 8.45, Ar-*H*), 7.70 (1H, d, J 5.30, Ar-*H*), 7.67-7.52 (5H, Ar-*H*), 7.40-7.30 (4H, Ar-*H*), 7.08 (1H, d, J 9.10, Ar-*H*), 6.84-6.76 (3H, Ar-*H*), 6.67-6.55 (4H, Ar-*H*), 6.47-6.37 (4H, Ar-*H*), 6.22 (1H, s, Ar-*H*), 6.15-6.12 (2H, Ar-*H*), 6.05-6.03 (2H, Ar-*H*), 5.73-5.60 (4H, Ar-*H*), 5.52 (1H, s, Ar-*H*), 5.48 (1H, Ar-*H*), 5.33 (1H, d, J 8.65, Ar-*H*), 5.15 (1H, Ar-*H*), 5.10 (1H, s, Ar-*H*), 4.77 (1H, d, J 8.45, Ar-*H*), 4.65 (1H, s, Ar-*H*), 4.14 (1H, d, J 7.50, Ar-*H*), 3.83 (1H, d, J 8.70, Ar-*H*), 3.78 (1H, d, J 10.15, Ar-*H*); ^{13}C { ^1H } NMR (125 MHz, CD_3CN): 177.45, 176.90, 176.78, 176.62, 176.50, 176.39, 176.00, 175.67, 175.55, 175.33, 175.09, 159.37, 159.24, 159.20, 159.13, 159.06, 158.94, 158.72, 158.63, 157.57, 157.14, 156.77, 156.49, 150.44, 150.14, 149.64, 149.36, 149.17, 148.84, 148.22, 148.11, 147.87, 141.24, 141.00, 140.98, 140.83, 140.80, 140.78, 140.73, 140.70, 140.69, 140.49, 133.05, 132.80, 132.75, 132.68, 132.55, 132.45, 132.43, 132.36, 132.21, 132.13, 131.98, 131.86, 131.80, 131.63, 131.58, 131.50, 131.47, 131.44, 131.38, 131.34, 131.30, 131.24, 131.17, 131.14, 131.12, 131.08, 131.04, 131.01, 130.95, 130.92, 130.88, 130.83, 130.79, 130.76, 130.73, 130.55, 130.52, 130.06, 129.92, 129.67, 129.48, 129.26, 129.15, 128.90, 127.67, 126.54, 126.38, 126.29, 126.19, 125.65, 125.46, 123.64, 122.43, 122.17, 122.00, 121.56, 120.84, 120.54, 120.19, 119.97, 119.95, 119.89, 119.85; ESI-MS: [**1b**(OTf)] $^{7+}$ 384.34, [**1b**(OTf) $_2$] $^{6+}$ 473.19, [**1b**(OTf) $_3$] $^{5+}$ 597.83, [**1b**(OTf) $_4$] $^{4+}$ 784.49, [**1b**(OTf) $_5$] $^{3+}$ 1095.62. Found: C, 49.05; H, 2.96; N, 7.95 %. Calc. for $\text{C}_{164}\text{H}_{108}\text{F}_{24}\text{Fe}_4\text{N}_{24}\text{O}_{24}\text{S}_8 \cdot 14.5\text{H}_2\text{O}$: C, 49.30; H, 3.46; N, 8.41 %.

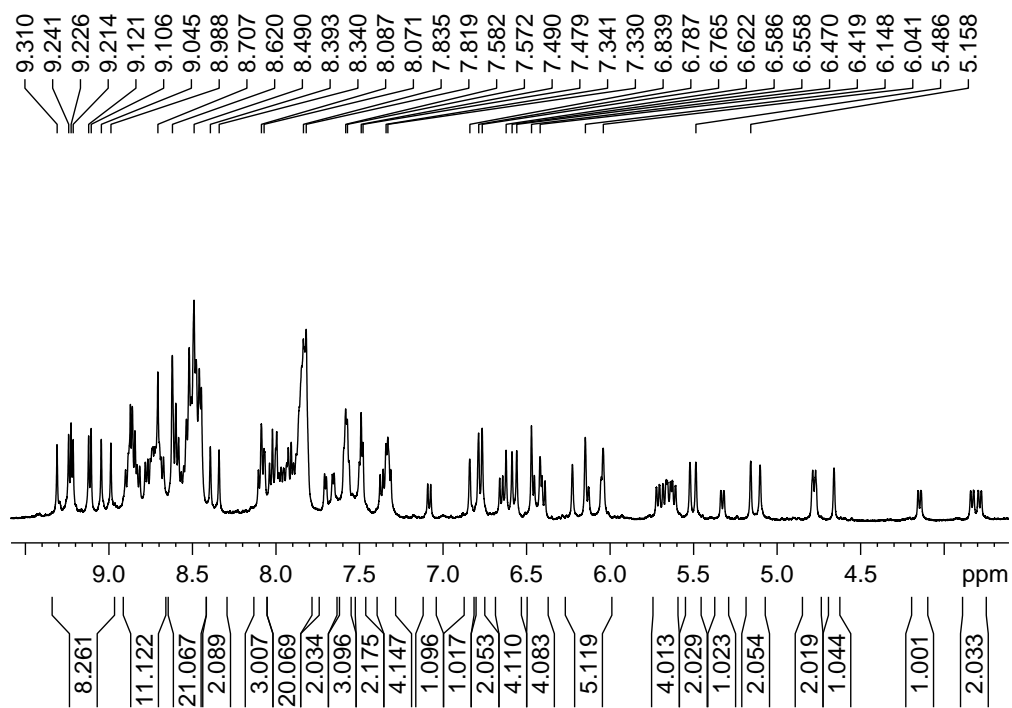


Figure S13. ^1H NMR spectrum for **1b**·OTf.

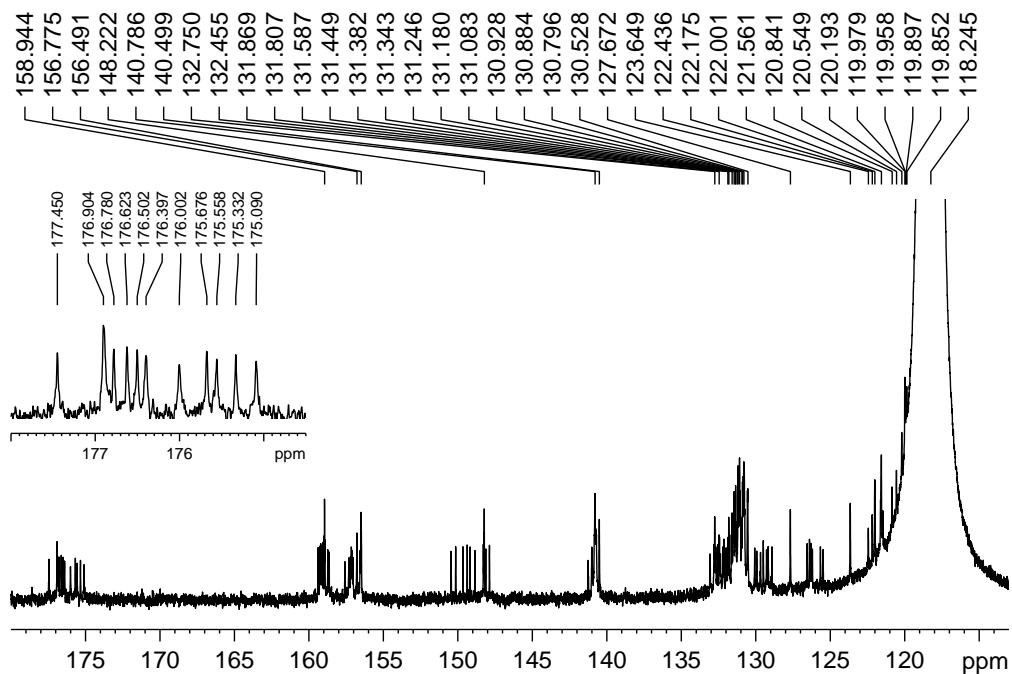


Figure S14. ^{13}C NMR spectrum for **1b**·OTf.

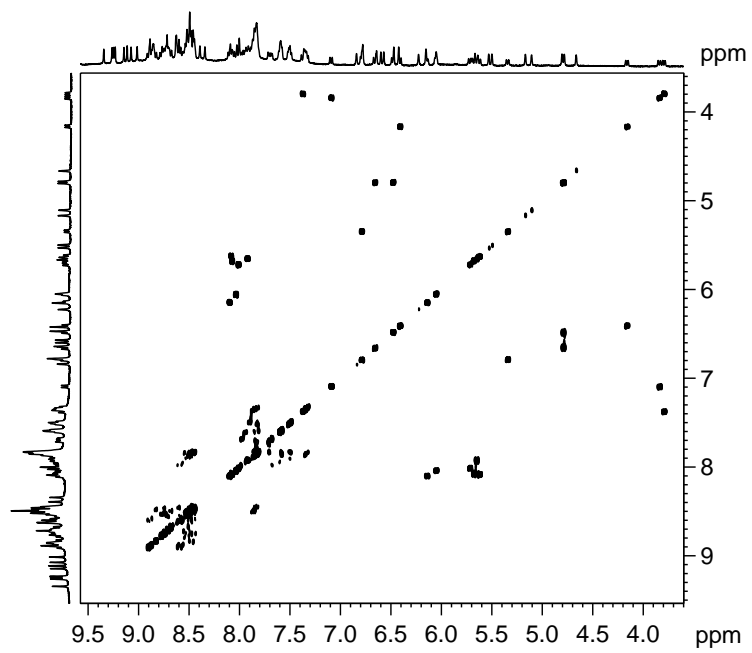


Figure S15. ^1H - ^1H COSY spectrum for **1b**·OTf.

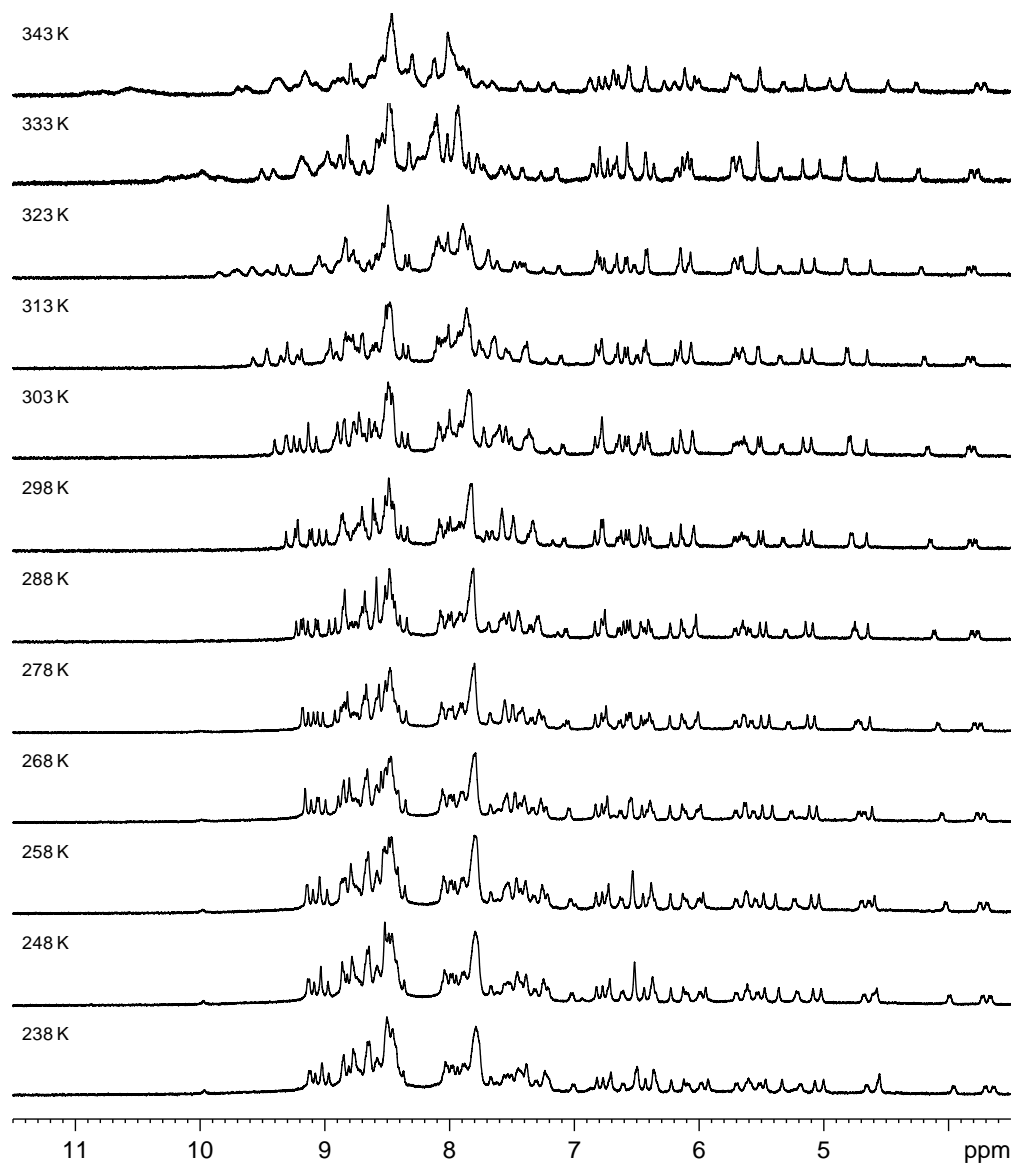
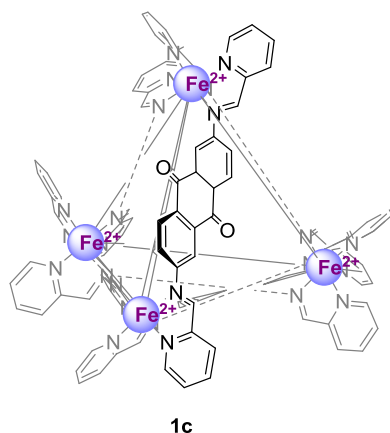


Figure S16. Variable temperature ^1H NMR spectrum for $\mathbf{1b}\cdot\text{OTf}$.



Synthesis of 1c·OTf. 2,6-diaminoanthraquinone **C** (50 mg, 0.21 mmol, 3 equiv.), 2-pyridinecarboxaldehyde (40 μ L, 0.42 mmol, 6 equiv.) and Fe(OTf)₂ (50 mg, 0.14 mmol, 2 equiv.) were mixed in MeCN (10 mL). The resulting solution was heated at 50°C for 12 hrs. Diethyl ether was added to precipitate the solid. The mixture was centrifuged and the solvent was decanted. The solid was dried and high vacuum to give the desired product **1c**·OTf as dark purple solid (93 mg, 68%). ¹H NMR (CD₃CN, 400 MHz): 9.43 (1H, s, imine-*H*), 9.38 (1H, s, imine-*H*), 9.33 (1H, s, imine-*H*), 9.28 (1H, s, imine-*H*), 9.27 (1H, s, imine-*H*), 9.17 (1H, s, imine-*H*), 9.06 (1H, s, imine-*H*), 8.91 (2H, s, imine-*H*), 8.90-8.45 (25H, Ar-*H*), 8.27-8.20 (4H, Ar-*H*), 8.16 (1H, d, *J* 8.36, Ar-*H*), 8.08 (1H, d, *J* 8.20, Ar-*H*), 8.05-7.70 (15H, Ar-*H*), 7.65-7.52 (9H, Ar-*H*), 7.50-7.32 (5H, Ar-*H*), 7.23 (1H, d, *J* 8.20, Ar-*H*), 6.90 (1H, s, Ar-*H*), 6.82 (1H, s, Ar-*H*), 6.51 (2H, Ar-*H*), 6.46 (1H, d, *J* 1.72, Ar-*H*), 6.42 (1H, d, *J* 7.88, Ar-*H*), 6.34 (1H, d, *J* 6.28, Ar-*H*), 6.21 (1H, s, Ar-*H*), 6.15 (1H, s, Ar-*H*), 6.10-6.06 (2H, Ar-*H*), 5.94-5.86 (4H, Ar-*H*), 5.77-5.73 (3H, Ar-*H*), 5.61 (1H, s, Ar-*H*), 5.40-5.34 (2H, Ar-*H*), 4.72 (1H, dd, *J* 8.12, 1.76, Ar-*H*), 4.29 (1H, d, *J* 6.88, Ar-*H*), 4.21 (1H, d, *J* 8.32, Ar-*H*); ¹³C {¹H} NMR (125 MHz, CD₃CN): 181.47, 181.21, 180.91, 180.18, 180.15, 180.11, 179.92, 179.86, 179.80, 179.45, 178.96, 177.25, 177.04, 176.89, 176.77, 176.64, 176.57, 176.36, 176.30, 176.19, 175.96, 157.80, 157.72, 157.66, 157.63, 157.55, 157.50, 157.23, 157.15, 157.05, 156.91, 156.85, 156.52, 156.44, 156.39, 156.30, 155.98, 155.90, 155.15, 155.06, 154.96, 154.70, 154.53, 154.25, 153.88, 153.82, 153.56, 140.24, 140.20, 140.11, 140.08, 139.98, 139.92, 139.80, 136.43, 135.93, 135.70, 135.60, 134.22, 134.17, 133.99, 133.91, 133.83, 133.75, 133.60, 133.45, 133.32, 133.02, 132.89, 132.71, 132.60, 132.54, 132.48, 132.20, 132.13, 132.02, 131.96, 131.79, 131.67, 131.64, 131.50, 131.46, 131.37, 131.30, 131.11, 130.85, 130.58, 130.53, 130.41, 130.29, 129.91, 129.79, 129.36, 129.21, 129.19, 129.01, 128.86, 128.02, 127.90, 127.73, 127.42, 126.84, 126.54, 126.22, 126.10, 126.01, 125.98, 125.79, 120.97, 120.43, 120.28, 120.13, 119.55, 119.19, 119.12, 119.03, 118.96, 118.80, 118.38, 118.02; ESI-MS: [**1c**(OTf)₄]⁴⁺ 829.50, [**1c**(OTf)₅]³⁺ 1155.66. Found: C, 47.28; H, 2.70; N, 7.80 %. Calc. for C₁₆₄H₉₆F₂₄Fe₄N₂₄O₃₆S₈·13H₂O: C, 47.48; H, 2.96; N, 8.10 %.

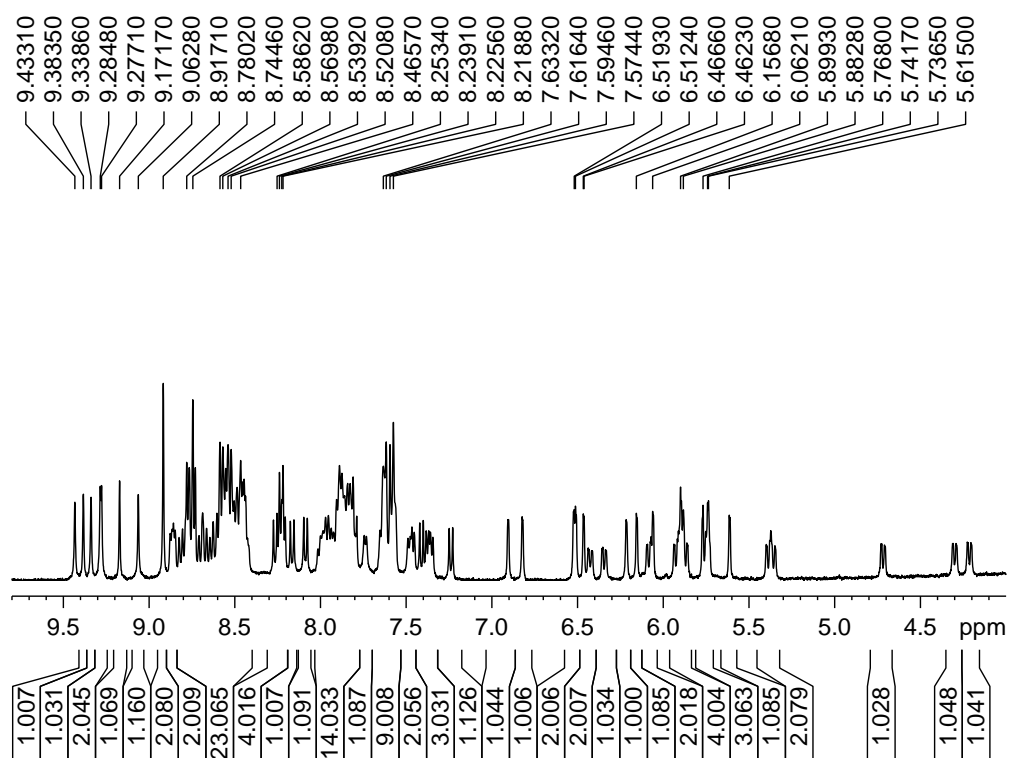


Figure S17. ^1H NMR spectrum for **1c**·OTf.

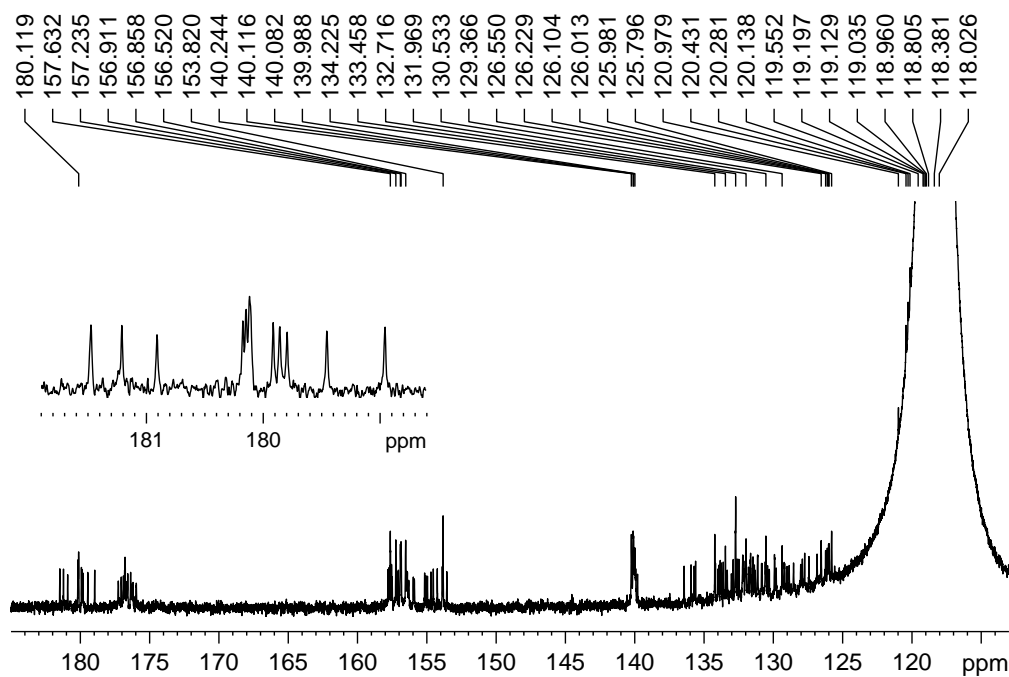


Figure S18. ^{13}C NMR spectrum for **1c**·OTf.

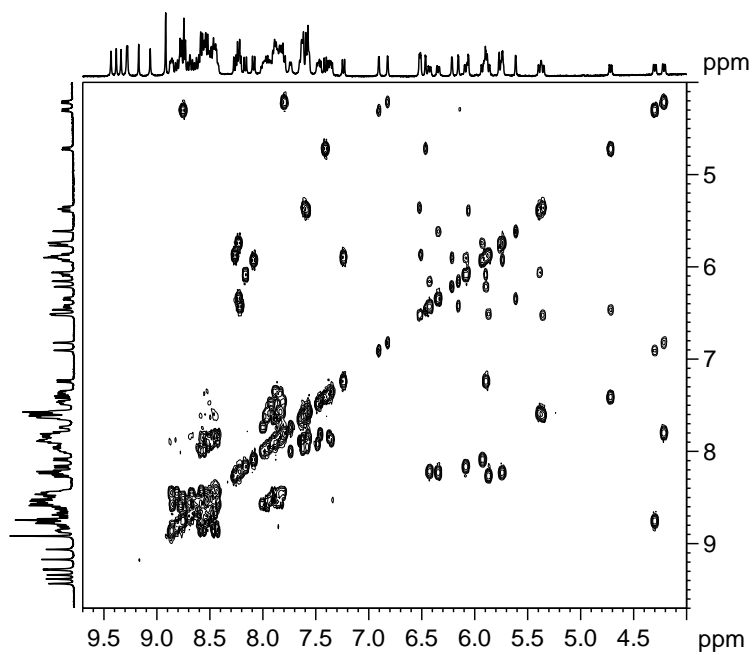


Figure S19. ^1H - ^1H COSY spectrum for **1c**·OTf.

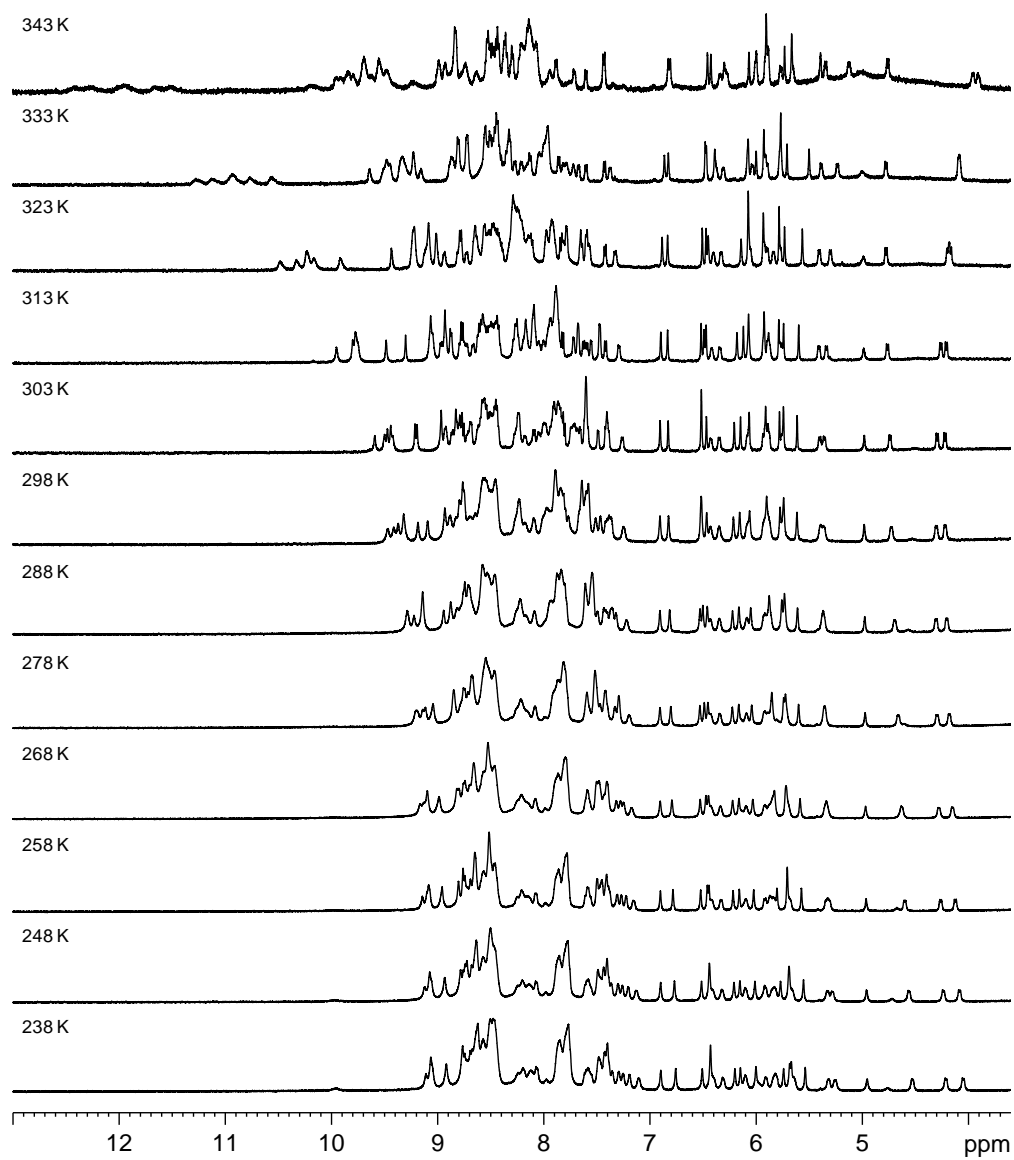
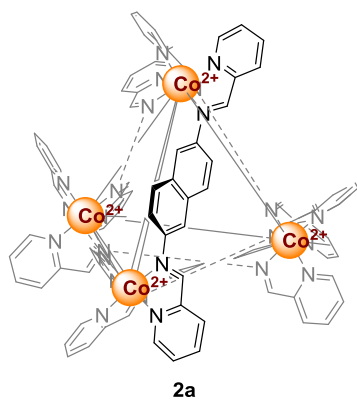


Figure S20. Variable temperature ^1H NMR spectrum for **1c**·OTf.



Synthesis of $2\mathbf{a}\cdot\text{BF}_4$. **A** (3.0 mg, 19 μmol , 3 equiv.), 2-pyridinecarboxaldehyde (3.6 μL , 37.9 μmol , 6 equiv.) and $\text{Co}(\text{BF}_4)_2$ (4.3 mg, 12.6 μmol , 2 equiv.) were mixed in MeCN (3 mL). The resulting solution was heated at 50°C for 12 hrs. Diethyl ether was added to precipitate the solid. The mixture was centrifuged and the solvent was decanted. The solid was dried and high vacuum to give the desired product $2\mathbf{a}\cdot\text{BF}_4$ as yellow solid (7.2 mg, 77%). ^1H NMR (CD_3CN , 400 MHz): 277.99 (1H, br, naphthalene-*H*), 271.50 (1H, br, naphthalene-*H*), 264.68 (1H, br, naphthalene-*H*), 243.33 (1H, br, imine-*H*), 238.26 (2H, br, imine-*H*), 237.40 (2H, br, imine-*H*), 234.35 (1H, br, imine-*H*), 230.37 (4H, br, imine-*H*), 218.65 (1H, br, imine-*H*), 216.30 (1H, br, imine-*H*), 122.85 (1H, br, py-*H*), 107.54 (1H, br, py-*H*), 92.19 (1H, br, py-*H*), 84.20 (1H, br, py-*H*), 77.73-69.97 (py-*H*), 63.96 (br, py-*H*), 62.42 (1H, br, py-*H*), 55.50 (1H, br, py-*H*), 54.36 (1H, br, py-*H*), 53.44 (1H, br, py-*H*), 52.63 (1H, br, py-*H*), 52.29 (1H, br, py-*H*), 51.36 (1H, br, py-*H*), 49.77 (1H, br, py-*H*), 49.43 (1H, br, py-*H*), 49.05 (1H, br, py-*H*), 48.55 (1H, br, py-*H*), 47.79 (1H, br, py-*H*), 47.18 (1H, br, py-*H*), 17.71-13.30 (12H, py-*H*), -10.38 (1H, br, py-*H*), -17.03 (1H, br, py-*H*), -29.59 (1H, br, py-*H*), -33.06 (1H, br, py-*H*), -37.64 (1H, br, py-*H*), -43.47 (1H, br, py-*H*), -53.83 (1H, br, py-*H*), -57.56 (1H, br, py-*H*); ESI-MS: $[\mathbf{2a}(\text{BF}_4)]^{7+}$ 334.46, $[\mathbf{2a}(\text{BF}_4)_2]^{6+}$ 404.55, $[\mathbf{2a}(\text{BF}_4)_3]^{5+}$ 502.83, $[\mathbf{2a}(\text{BF}_4)_4]^{4+}$ 650.30, $[\mathbf{2a}(\text{BF}_4)_5]^{3+}$ 896.04, $[\mathbf{2a}(\text{BF}_4)_6]^{2+}$ 1387.52. Found: C, 49.23; H, 3.40; N, 11.00 %. Calc. for $\text{C}_{132}\text{H}_{96}\text{B}_8\text{Co}_4\text{F}_{32}\text{N}_{24}\cdot 14.14\text{H}_2\text{O}$: C, 49.49; H, 3.91; N, 10.49 %.

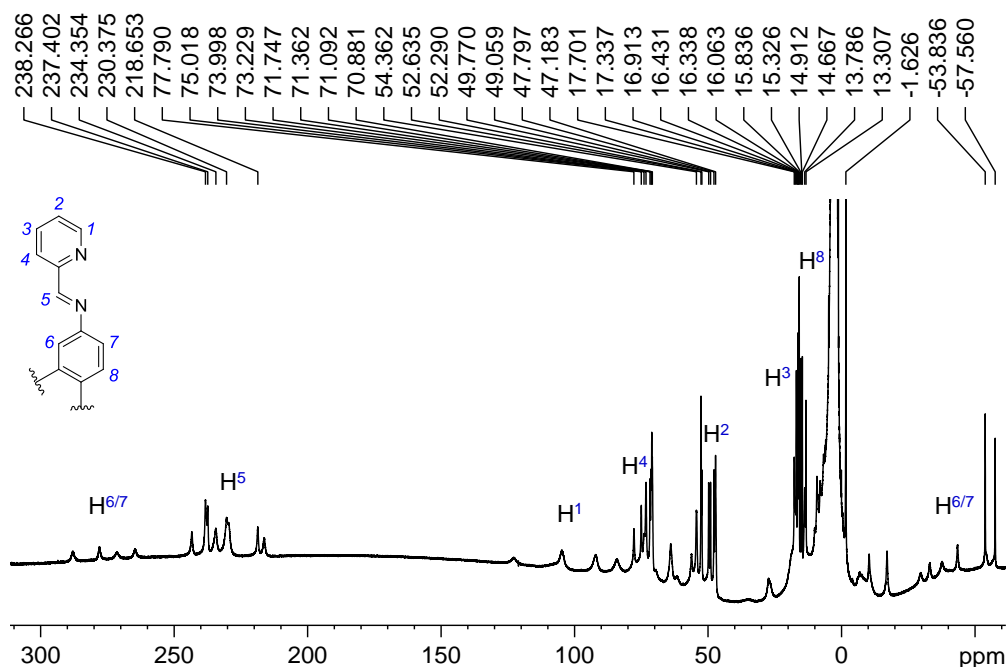


Figure S21. ^1H NMR spectrum for $2\mathbf{a}\cdot\text{BF}_4$.

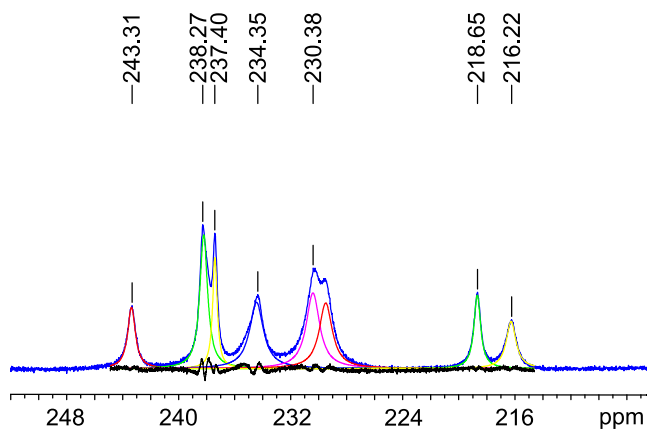


Figure S22. Deconvolution analysis of imine proton region.

Table S1. Deconvolution analysis of the imine proton region showing there are 12 imines in total.

Peak No.	ppm	Relative integration
1	243.37	1.03
2	238.21	2.27
3	237.41	1.12
4	234.44	2.01
5	230.40	2.21
6	229.49	1.88
7	218.67	1.07
8	216.25	1.00

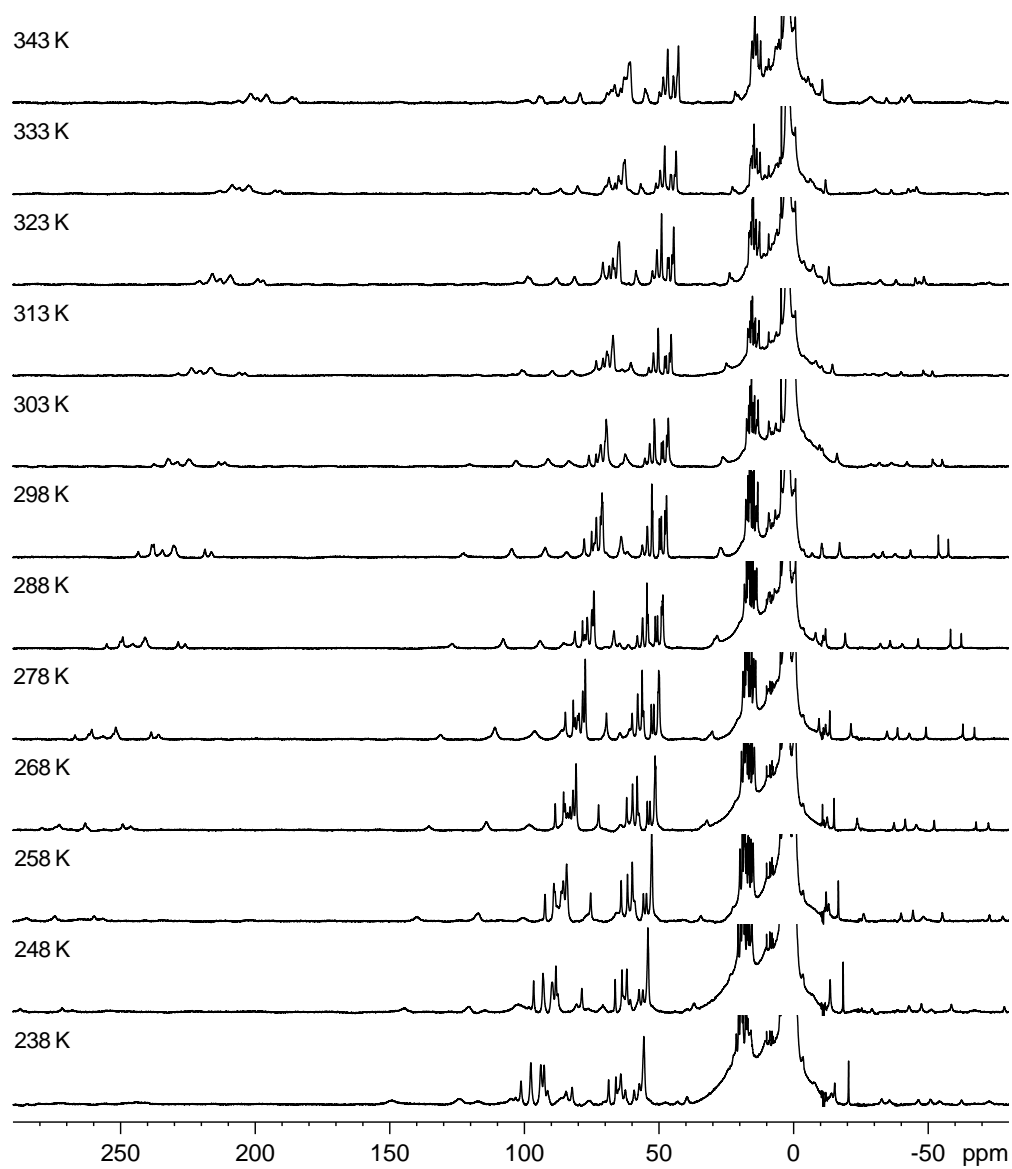


Figure S23. Variable temperature ^1H NMR spectrum for $2\mathbf{a}\cdot\text{BF}_4$.

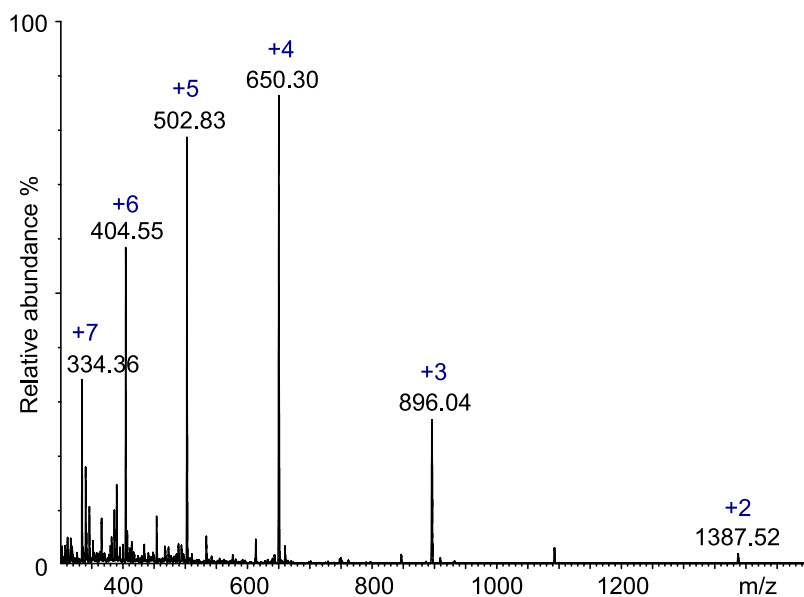
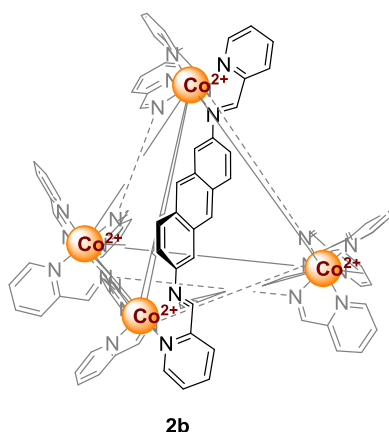


Figure S24. ESI-MS spectrum for **2a**·BF₄.



Synthesis of 2b·BF₄. **B** (4.0 mg, 19.2 μmol, 3 equiv.), 2-pyridinecarboxaldehyde (3.6 μL, 38.4 μmol, 6 equiv.) and Co(BF₄)₂·6H₂O (4.4 mg, 12.8 μmol, 2 equiv.) were mixed in MeCN (2 mL). The resulting solution was heated at 50°C for 4 hrs. Diethyl ether was added to precipitate the solid. The mixture was centrifuged and the solvent was decanted. The solid was dried and high vacuum to give the desired product **2b**·BF₄ as orange solid (6.6 mg, 63%). ¹H NMR (CD₃CN, 400 MHz): 242.66 (1H, br, imine-*H*), 237.79 (1H, br, imine-*H*), 230.59 (1H, br, imine-*H*), 100-48 (9H, br, py-*H*), 20-10 (4H, br, imine-*H*); ESI-MS: [**2b**(BF₄)₇]⁷⁺ 337.21, [**2b**(BF₄)₂]⁶⁺ 454.59, [**2b**(BF₄)₃]⁵⁺ 562.85, [**2b**(BF₄)₄]⁴⁺ 725.28, [**2b**(BF₄)₅]³⁺ 996.07. Found: C, 52.78; H, 3.76; N, 10.03 %. Calc. for C₁₅₆H₁₀₈B₈Co₄N₂₄F₃₂·16H₂O: C, 52.97; H, 3.99; N, 9.50 %.

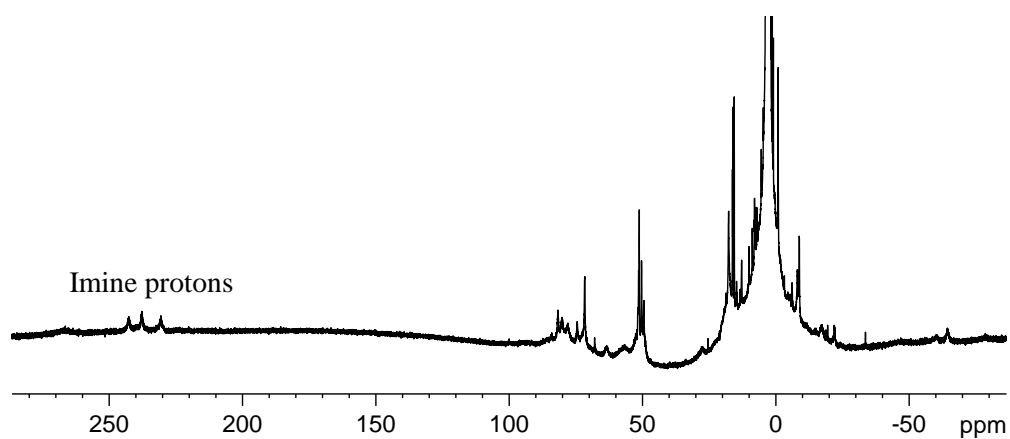


Figure S25. ^1H NMR spectrum for $2\mathbf{b}\cdot\text{BF}_4$.

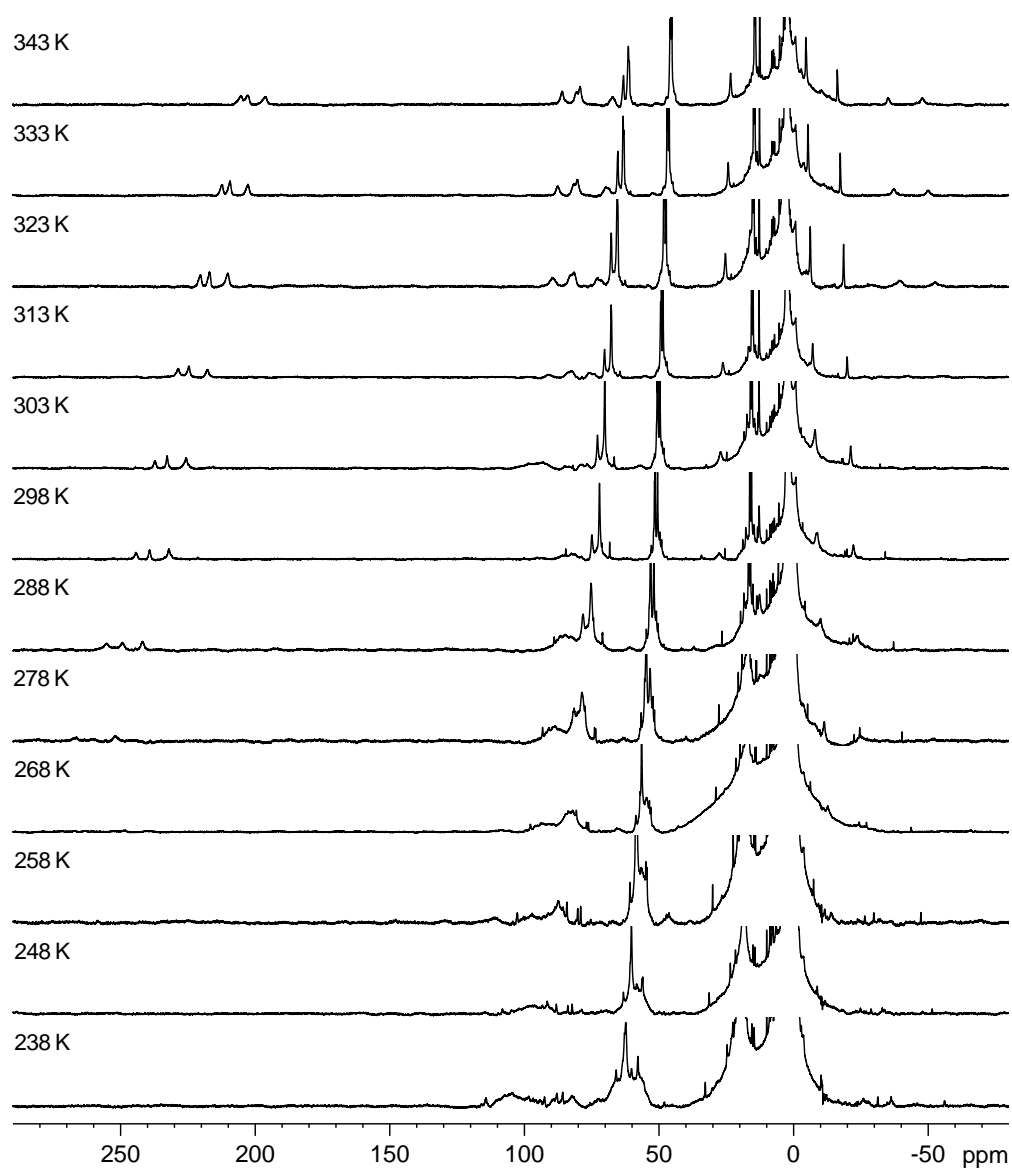
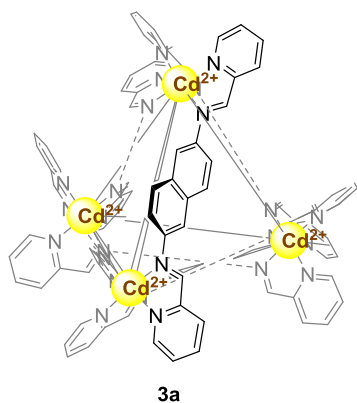


Figure S26. Variable temperature ^1H NMR spectrum for $2\mathbf{b}\cdot\text{BF}_4$.



Synthesis of 3a·ClO₄. **A** (5.0 mg, 31.5 μmol, 3 equiv.), 2-pyridinecarboxaldehyde (6.0 μL, 63.3 μmol, 6 equiv.) and Cd(ClO₄)₂ (6.5 mg, 21.0 μmol, 2 equiv.) were mixed in MeCN (3 mL). The resulting solution was heated at 50°C for 12 hrs. Diethyl ether was added to precipitate the solid. The mixture was centrifuged and the solvent was decanted. The solid was dried and high vacuum to give the desired product **3a**·ClO₄ as yellow solid (12.2 mg, 71%). ¹H NMR (CD₃CN, 400 MHz): 9.08 (4H, t, *J*_{Cd-H} 17.68, imine-*H*), 9.07 (4H, t, *J*_{Cd-H} 20.00, imine-*H*), 8.63 (4H, d, *J* 7.76, 3-py-*H*), 8.60 (4H, d, *J* 4.36, 6-py-*H*), 8.53 (4H, t, *J* 7.78, 4-py-*H*), 8.43 (4H, t, *J*_{Cd-H} 19.36, imine-*H*), 8.40-8.36 (8H, 4-py-*H*), 8.31 (4H, d, *J* 7.78, 3-py-*H*), 8.13 (4H, d, *J* 4.20, 6-py-*H*), 8.0 (8H, d, 6-py-*H* and 3-py-*H*), 7.99 (4H, t, *J* 5.80, 5-py-*H*), 7.89 (4H, m, 5-py-*H*), 7.80 (4H, t, *J* 5.74, 5-py-*H*), 7.54 (4H, s, 1-naph-*H*), 7.49 (4H, d, *J* 8.80, 4-naph-*H*), 7.28 (4H, dd, *J* 8.76, 1.96, 3-naph-*H*), 7.21 (4H, d, *J* 8.84, 4-naph-*H*), 6.69 (4H, s, 1-naph-*H* of *anti* ligand), 6.51 (4H, br, 4-naph-*H* of *anti* ligand), 6.39 (4H, dd, *J* 8.72, 2.04, 3-naph-*H*), 6.31 (4H, s, 1-naph-*H*), 5.88 (4H, d, *J* 8.64, 3-naph-*H* of *anti* ligand); ¹³C {¹H} NMR (125 MHz, CD₃CN): 166.87, 166.21, 164.19, 152.11, 151.73, 151.26, 147.64, 147.45, 147.40, 147.30, 146.71, 145.98, 143.44, 143.35, 143.11, 133.59, 133.27, 133.06, 132.27, 132.46, 131.54, 131.12, 130.96, 129.95, 129.84, 122.53, 121.71, 121.53, 120.90, 120.15, 119.43; ESI-MS: [**3a**(ClO₄)₄]⁴⁺ 716.98, [**3a**(ClO₄)₅]³⁺ 989.27. Found: C, 47.97; H, 3.00; N, 9.96 %. Calc. for C₁₃₂H₉₆Cl₈Cd₄N₂₄O₃₂·2H₂O: C, 48.05; H, 3.05; N, 10.19 %.

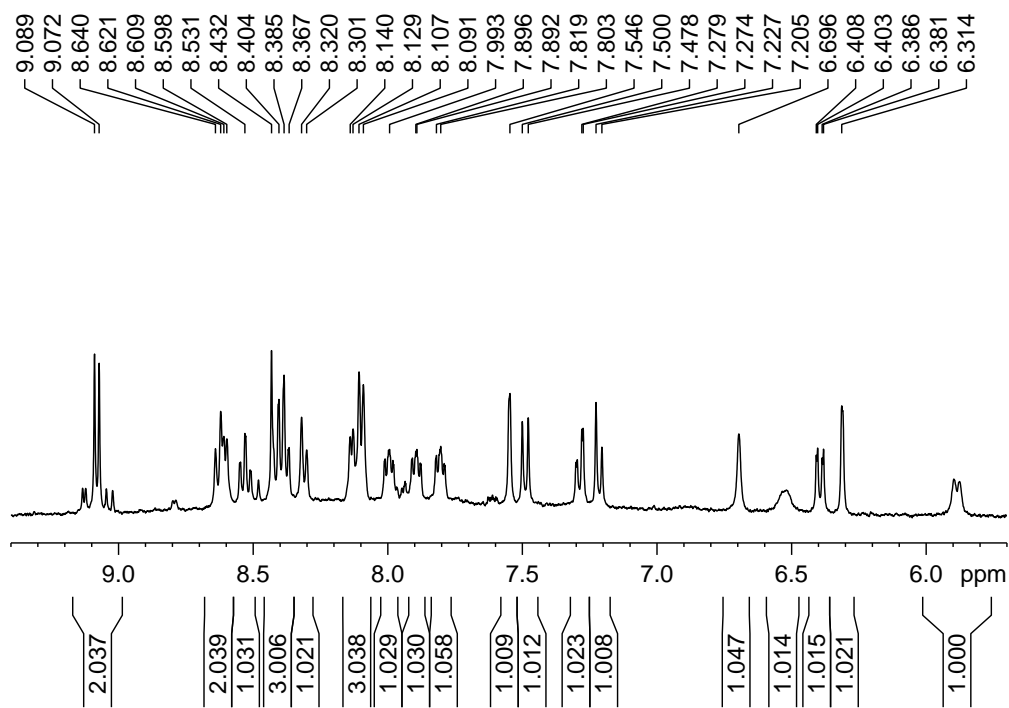


Figure S27. ^1H NMR spectrum for $3\mathbf{a}\cdot\text{ClO}_4$.

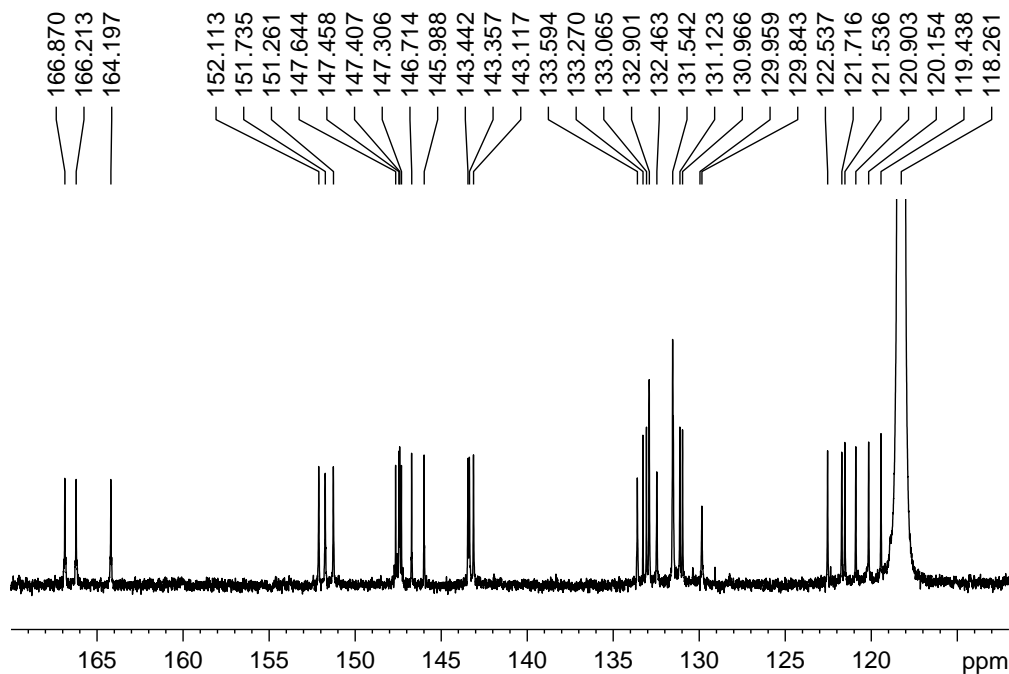


Figure S28. ^{13}C NMR spectrum for $3\mathbf{a}\cdot\text{ClO}_4$.

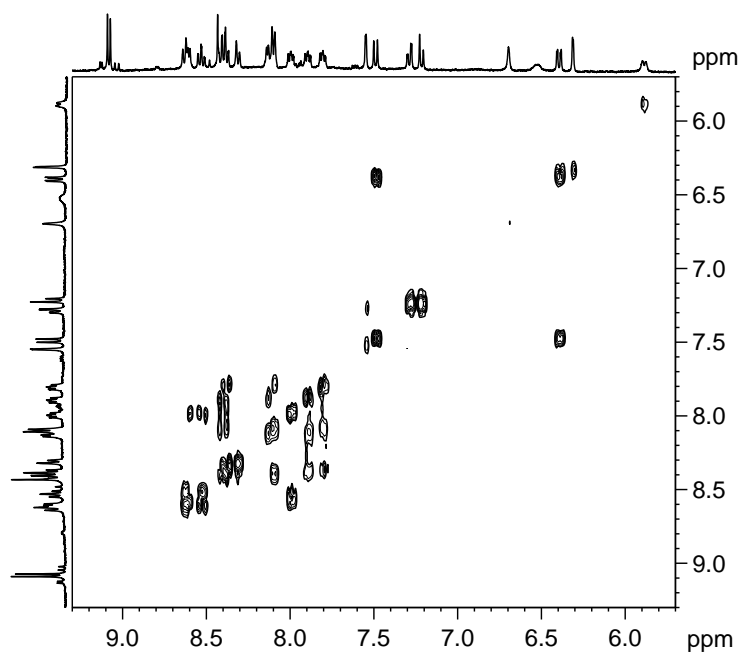


Figure S29. ^1H - ^1H COSY spectrum for **3a**·ClO₄.

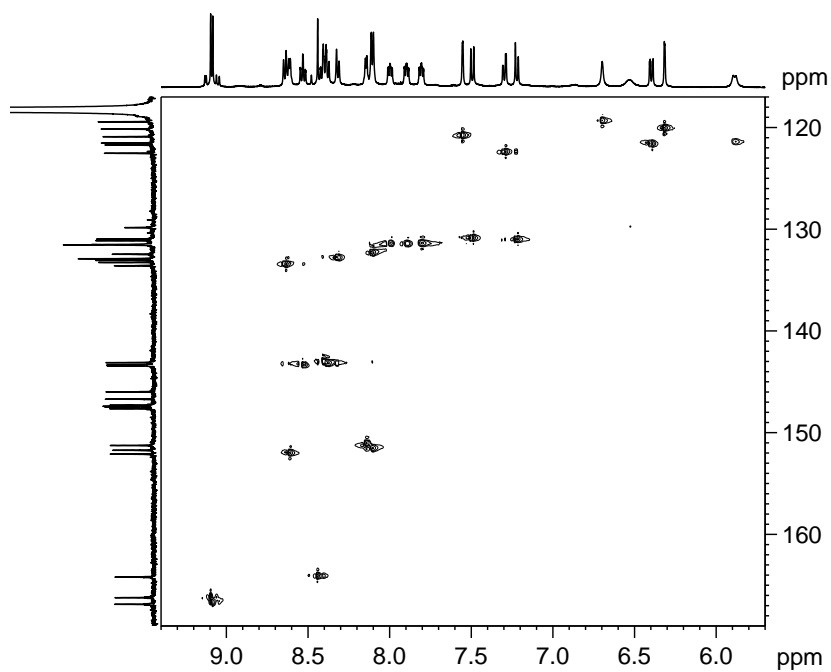


Figure S30. ^1H - ^{13}C HMQC spectrum for **3a**·ClO₄.

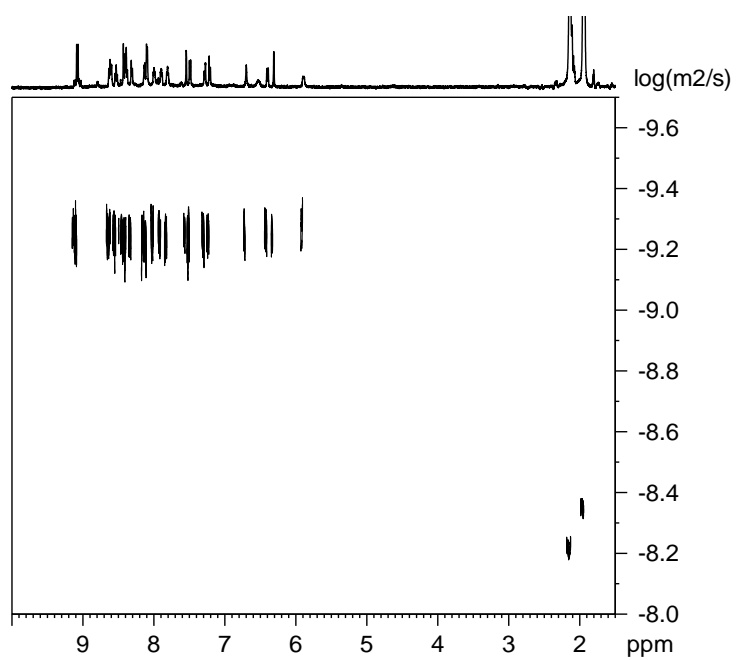


Figure S31. DOSY spectrum for **3a**·ClO₄. $r_H = 10.8 \text{ \AA}$.

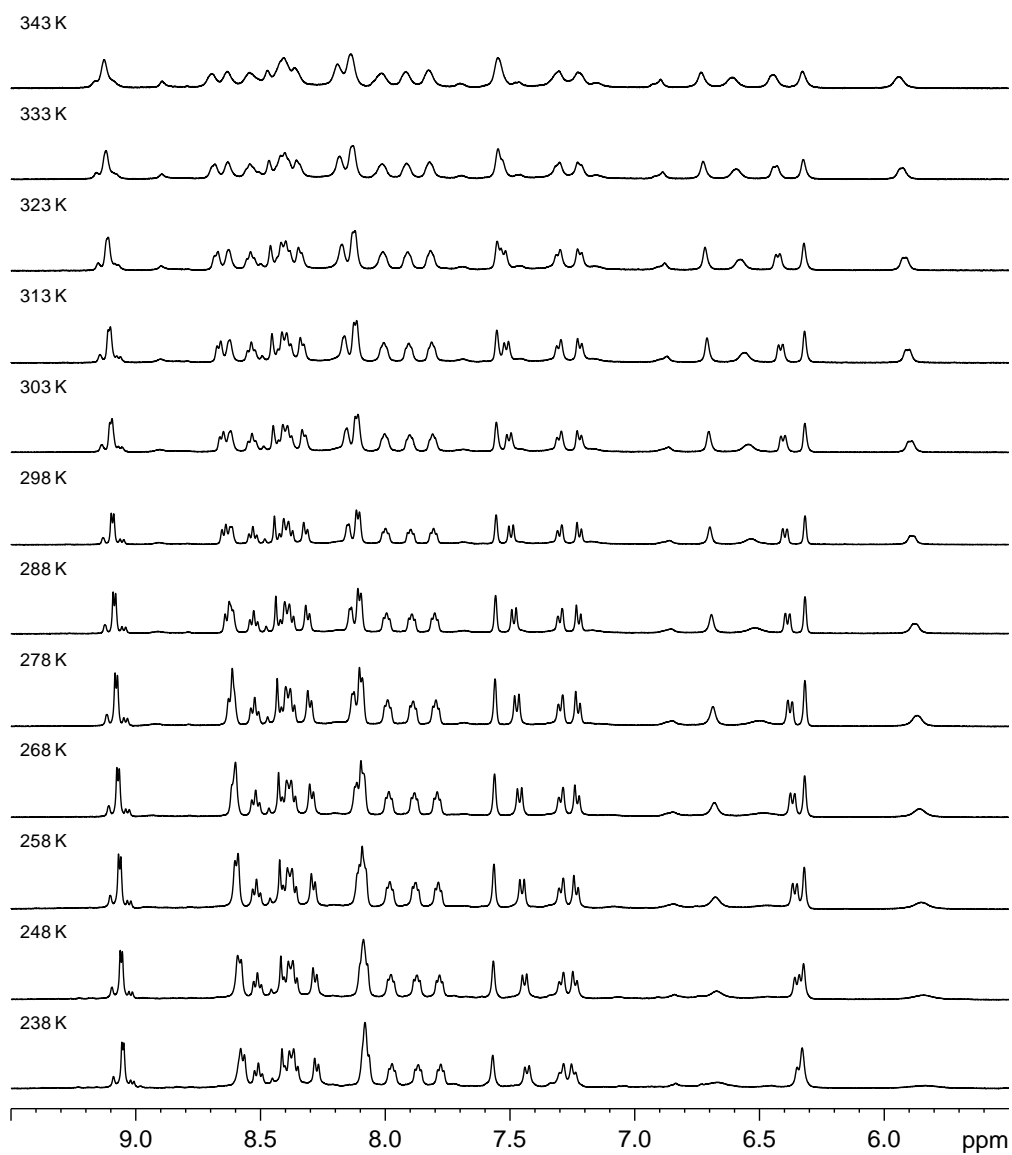


Figure S32. Variable temperature ¹H NMR spectrum for **3a**·ClO₄.

Crystallography

Crystals were grown by vapour diffusion of diethyl ether into acetonitrile or nitromethane solutions of the complexes.

Data for **1a**·8ClO₄·4NO₂Me were collected at Beamline I19 of Diamond Light Source employing silicon double crystal monochromated synchrotron radiation (0.6889 Å) with ω scans at 100(2) K. (S3) Data integration and reduction for were undertaken with CrystalClear (S3). A multi-scan empirical absorption correction was applied to the data using CrystalClear (S3). Data for **1a**·8OTf·4MeCN were collected on a Oxford Gemini Ultra employing confocal mirror monochromated Cu-K α radiation generated from a sealed tube (1.5418 Å) with ω and ψ scans at 120(2) K (S4). Data integration and reduction were undertaken with CrysAlisPro (S4). Gaussian and multi-scan empirical absorption corrections were applied to the data using CrysAlisPro (S4). Data for **2a**·8BF₄·5NO₂Me and **2a**·8BF₄·3MeCN were collected on a Nonius Kappa FR590 diffractometer employing graphite-monochromated Mo-K α radiation generated from a sealed tube (0.71073 Å) with ω and ψ scans at 180(2) K. Data integration and reduction were undertaken with HKL Denzo and Scalepack (S5). Multi-scan empirical absorption corrections were applied to the data set using SORTAV (S6, 7).

Subsequent computations for all structures were carried out using the WinGX-32 graphical user interface (S8). Structures were solved using SUPERFLIP (S9) then refined and extended with SHELXH-97 (S10). In general, non-hydrogen atoms with occupancies greater than 0.5 were refined anisotropically. Carbon-bound hydrogen atoms were included in idealised positions and refined using a riding model. Disorder was modelled using standard crystallographic methods including constraints, restraints and rigid bodies where necessary. Crystallographic data along with specific details pertaining to the refinement follow (CCDC 901947 - 901951).

1a·8ClO₄·4NO₂Me

Formula C₁₃₆H₁₀₈Cl₈Fe₄N₂₈O₄₀, M 3281.50, triclinic, space group *P*-1(#2), a 20.494(8), b 21.095(8), c 22.710(8) Å, α 68.231(16), β 65.485(14), γ 82.91(2)°, V 8290(5) Å³, *D*_c 1.315 g cm⁻³, Z 2, crystal size 0.15 by 0.08 by 0.04 mm, colour purple, habit block temperature 100(2) Kelvin, λ (synchrotron) 0.68890 Å, μ (synchrotron) 0.552 mm⁻¹, *T*(CRYSTALCLEAR)_{min,max} 0.9218, 0.9783, $2\theta_{\max}$ 40.30, hkl range -20 20, -21 21, -22 22, *N* 73909, *N*_{ind} 17278 (*R*_{merge} 0.0541), *N*_{obs} 13471 (*I* > 2 σ (*I*)), 1883 parameters, residuals* *R*1(*F*) 0.1117, *wR*2(*F*²) 0.3196, GoF(all) 1.004, $\Delta\rho_{\min,\max}$ -1.046, 1.584 e⁻ Å⁻³.

* *R*1 = $\sum||F_o| - |F_c||/\sum|F_o|$ for *F*_o > 2 σ (*F*_o); *wR*2 = $(\sum w(F_o^2 - F_c^2)^2/\sum wF_c^2)^{1/2}$ all reflections

$$w=1/[\sigma^2(F_o^2)+(0.2000P)^2+30.000P] \text{ where } P=(F_o^2+2F_c^2)/3$$

Specific Details:

These crystals were extremely unstable, rapidly decaying once removed from the mother liquor and required rapid handling at dry-ice temperatures (< 5 s) to facilitate data collection. The crystals were also weakly diffracting with very few reflections recorded at higher than 1.0 Å. All eight tetrafluoroborate anions show positional disorder (either the whole molecule or some of the fluorine atoms) and were modelled in two parts. Restraints were applied to the bond lengths and thermal parameters of the disordered atoms to ensure a reasonable refinement. Bond length restraints were also applied to some of the nitromethane solvent molecules. The four nitromethane molecules are located over 1 full occupancy site and 6 half occupancy sites. The SQUEEZE (S11) function of PLATON (S12) was employed to remove the contribution of the electron density associated with further disordered solvent molecules that could not be adequately modelled despite numerous attempts, resulting in more satisfactory residuals. One of the central naphthalene groups is disordered over two conformations (corresponding to a 180° rotation of the naphthalene group about the C_{naph}-N_{imine} bonds). The disordered atoms were modelled with isotropic thermal parameters and rigid body restraints applied to ensure a reasonable geometry. An additional naphthalene unit (C95-C104) shows high thermal parameters indicative of thermal motion or some unresolved disorder which could not be modelled despite numerous attempts. This group was also refined with rigid body restraints. The remaining peaks of electron density (up to 1.584 e⁻ Å⁻³) are all close to the disordered anions and solvent molecules, possibly indicative of some further disorder which could not be resolved.

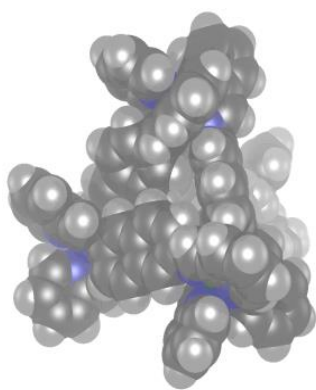


Figure S33. CPK presentation of the crystal structure of **1a**·8ClO₄·4MeNO₂, showing most cavity space is occupied by ligand.

1a·8OTf·4MeCN

Formula $C_{148}H_{122}F_{24}Fe_4N_{28}O_{26}S_8$, M 3644.62, monoclinic, space group C2/c (#15), a 35.2528(12), 19.0549(5), c 28.1655(11) Å, β 119.493(5), V 16468.1(13) Å³, D_c 1.470 g cm⁻³, Z 4, crystal size 0.38 by 0.32 by 0.32 mm, colour purple, habit block temperature 120(2) Kelvin, λ (CuK α) 1.54180 Å, μ (CuK α) 4.611 mm⁻¹, T (CRYALISPRO)_{min,max} 0.2732, 0.4303, $2\theta_{max}$ 50.43, hkl range -35 35, -19 15, -28 28, N 25223, N_{ind} 8516 (R_{merge} 0.0411), N_{obs} 8629 ($I > 2\sigma(I)$), 1009 parameters, residuals* $R1(F)$ 0.1107, $wR2(F^2)$ 0.3200, GoF(all) 1.034, $\Delta\rho_{min,max}$ -1.185, 1.401 e⁻ Å⁻³.

* $R1 = \sum||F_o| - |F_c||/\sum|F_o|$ for $F_o > 2\sigma(F_o)$; $wR2 = (\sum w(F_o^2 - F_c^2)^2/\sum wF_c^2)^{1/2}$ all reflections

$w=1/[\sigma^2(F_o^2)+(0.2000P)^2+200.000P]$ where $P=(F_o^2+2F_c^2)/3$

Specific Details:

The crystals were weakly diffracting with very few reflections recorded at higher than 1.0 Å resolution. The cage crystallises with crystallographic inversion symmetry such that the asymmetric unit comprises half of the tetrahedron. Two of the naphthyl groups are disordered over special positions such that the second positions of the disordered groups are generated from the symmetry equivalent of the first. The two positions of the disordered naphthyl groups represent two conformations of the ligand where the naphthyl spacer has been rotated by 180°. The disordered atoms were refined with isotropic thermal parameters and required the use of rigid body restraints to ensure a reasonable geometry. Two of the triflate anions show positional disorder and were modelled in two parts. Restraints were applied to the bond lengths and thermal parameters of the disordered atoms to ensure a reasonable refinement. Only the sulphur atoms of the disordered triflate anions were refined anisotropically. Hydrogen atoms were not applied to the acetonitrile solvent molecules and one of these was refined with isotropic thermal parameters. The SQUEEZE (S11) function of PLATON (S12) was employed to remove the contribution of the electron density associated with further disordered solvent molecules that could not be adequately modelled despite numerous attempts, resulting in more satisfactory residuals. The remaining peaks of electron density (up to 1.401 e⁻ Å⁻³) are all close to the disordered anions and solvent molecules, possibly indicative of some further disorder which could not be resolved.

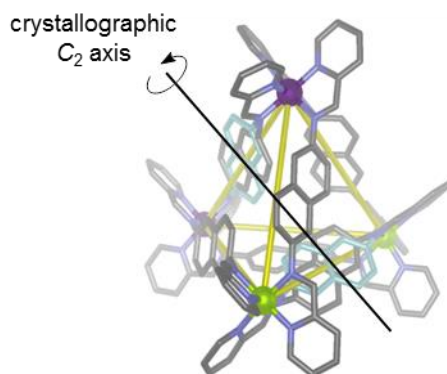


Figure S34. Crystal structure of **1a**·OTf. The naphthyl spacer within the *anti* ligands is disordered over two positions that are colored in grey and light blue. Counter anions, solvent molecules and hydrogen atoms are omitted for clarity.

2a·8BF₄·5NO₂Me

Formula C₁₃₇H₁₁₁B₈Co₄F₃₂N₂₉O₁₀, M 3253.75, triclinic, space group *P*-1(#2), a 16.476(3), b 21.246(4), c 27.807(6) Å, α 95.51(3), β 97.03(3), γ 111.25(3)°, V 8900(3) Å³, *D*_c 1.214 g cm⁻³, Z 2, crystal size 0.18 by 0.12 by 0.05 mm, colour orange, habit block, temperature 180(2) Kelvin, λ (MoK α) 0.71073 Å, μ (MoK α) 0.456 mm⁻¹, *T*(SORTAV)_{min,max} 0.870, 0.969, $2\theta_{\max}$ 41.64, hkl range -16 16, -21 21, -27 27, *N* 74151, *N*_{ind} 18556 (*R*_{merge} 0.0629), *N*_{obs} 13576 (*I* > 2 σ (*I*)), 1824 parameters, residuals* *R*1(*F*) 0.1018, *wR*2(*F*²) 0.3118, GoF(all) 1.253, $\Delta\rho_{\min,\max}$ -0.790, 1.006 e⁻ Å⁻³.

**R*1 = $\sum||F_o| - |F_c||/\sum|F_o|$ for $F_o > 2\sigma(F_o)$; *wR*2 = $(\sum w(F_o^2 - F_c^2)^2/\sum (wF_c^2)^2)^{1/2}$ all reflections

$w=1/[\sigma^2(F_o^2)+(0.2000P)^2]$ where $P=(F_o^2+2F_c^2)/3$

Specific Details:

The crystals were weakly diffracting with very few reflections recorded at higher than 0.9 Å resolution. Four of the eight tetrafluoroborate anions show positional disorder and were modelled in two parts. Restraints were applied to the bond lengths and thermal parameters of the disordered atoms to ensure a reasonable refinement. Three more of the tetrafluoroborate anions show high thermal parameters indicating thermal motion or some unresolved disorder which could not be modelled despite multiple attempts. These atoms were refined with isotropic thermal parameters and the B-F bond lengths restrained (DFIX) to follow the idealized geometry of a tetrafluoroborate anion. Bond length restraints were also applied to some of the nitromethane solvent molecules to ensure a

reasonable refinement. The five nitromethane molecules are located over 3 full occupancy sites and 4 half occupancy sites. The SQUEEZE (S11) function of PLATON (S12) was employed to remove the contribution of the electron density associated with further disordered solvent molecules that could not be adequately modelled despite numerous attempts, resulting in more satisfactory residuals.

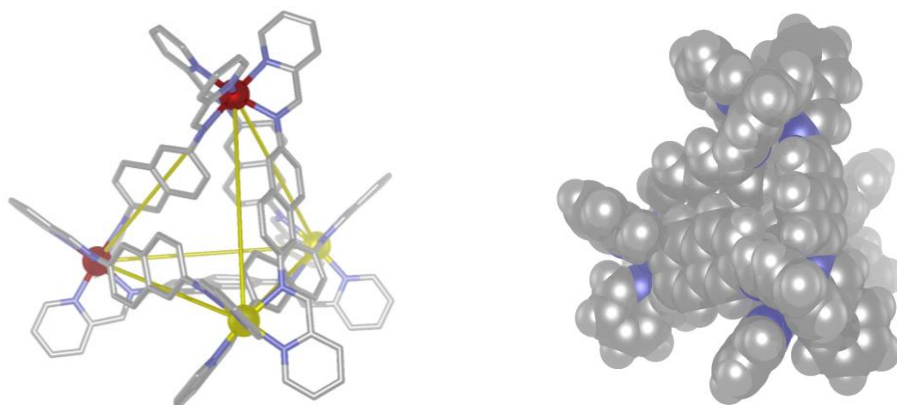


Figure S35. Crystal structure of **2a**·8BF₄·5NO₂Me. Left: ball and stick presentation the Co^{II} ions of identical stereochemistry are coloured the same. Right: cpk presentation of the cage showing that the ligands are so closely packed so as to eliminate cavity space.

2a·8BF₄·3MeCN

Formula C₁₃₈H₁₀₅B₈Co₄F₃₂N₂₇, M 3071.69, triclinic, space group *P*-1(#2), a 16.405(3), b 21.175(4), c 27.978(6) Å, α 95.86(3), β 97.14(3), γ 111.46(3), V 8860(3) Å³, *D*_c 1.151 g cm⁻³, Z 2, crystal size 0.20 by 0.15 by 0.05 mm, colour orange, habit block, temperature 180(2) Kelvin, λ (MoK α) 0.71073 Å, μ (MoK α) 0.450 mm⁻¹, *T*(SORTAV)_{min,max} 0.692, 0.970, $2\theta_{\max}$ 41.00, hkl range -16 15, -20 20, -25 27, *N* 27282, *N*_{ind} 14536 (*R*_{merge} 0.0649), *N*_{obs} 8306 (*I* > 2 σ (*I*)), 1639 parameters, residuals* *R*1(*F*) 0.1076, *wR*2(*F*²) 0.3232, GoF(all) 1.098, $\Delta\rho_{\min,\max}$ -0.624, 1.076 e⁻ Å⁻³.

**R*1 = $\sum||F_o| - |F_c||/\sum|F_o|$ for *F*_o > 2 σ (*F*_o); *wR*2 = $(\sum w(F_o^2 - F_c^2)^2/\sum w(F_c^2)^2)^{1/2}$ all reflections

$w=1/[\sigma^2(F_o^2)+(0.2000P)^2]$ where $P=(F_o^2+2F_c^2)/3$

Specific Details:

The crystals were weakly diffracting with very few reflections recorded at higher than 1.0 Å resolution. The tetrafluoroborate anions and acetonitrile solvent molecules were refined with isotropic thermal parameters and restraints were applied to the bond lengths to ensure a reasonable refinement. The SQUEEZE (S11) function of PLATON (S12) was employed to remove the contribution of the electron density associated with further disordered solvent molecules that could not be adequately modelled despite numerous attempts, resulting in more satisfactory residuals. A reasonable quality refinement was achieved despite less than ideal completeness (81.6 %) and the data is more than sufficient for establishing the connectivity of the structure. The structure of **2a** in **2a**·8BF₄·3MeCN is very similar in all respects to that of the better quality data set obtained for **2a**·8BF₄·5NO₂Me.

1b·8OTf·2Et₂O·3MeCN

Formula C₁₇₄H₁₃₅F₂₄Fe₄N₂₇O₂₅S₈, M 3939.97, triclinic, space group *P*-1(#2), *a* 18.800(6), *b* 18.903(6), *c* 27.051(9) Å, α 101.662(4), β 94.885(3), γ = 94.905(4)°, *V* 9328(5) Å³, *D_c* 1.403 g cm⁻³, *Z* 2, crystal size 0.10 by 0.05 by 0.02 mm, colour purple, habit block temperature 100(2) Kelvin, λ (synchrotron) 0.68890 Å, μ (synchrotron) 0.491 mm⁻¹, *T*(CRYSTALCLEAR)_{min,max} 0.9526, 0.9903, $2\theta_{\max}$ 40.30, hkl range -18 18, -18 18, -27 27, *N* 81258, *N*_{ind} 19376 (*R*_{merge} 0.0708), *N*_{obs} 15575 (*I* > 2σ(*I*)), 2054 parameters, residuals* *R1*(*F*) 0.0893, *wR2*(*F*²) 0.2671, GoF(all) 1.110, $\Delta\rho_{\min,\max}$ -1.426, 1.345 e⁻ Å⁻³.

**R1* = $\sum||F_o| - |F_c||/\sum|F_o|$ for *F_o* > 2σ(*F_o*); *wR2* = $(\sum w(F_o^2 - F_c^2)^2/\sum(wF_c^2)^2)^{1/2}$ all reflections

$w=1/[\sigma^2(F_o^2)+(0.182900P)^2+11.600400P]$ where $P=(F_o^2+2F_c^2)/3$

Specific Details:

The crystals were also weakly diffracting with very few reflections recorded at higher than 1.0 Å. Two of the triflate anions show positional disorder and were modelled in two parts. Restraints were applied to the bond lengths and thermal parameters of the disordered atoms to ensure a reasonable refinement. A further triflate is also disordered but only the sulfur atom of the second position could be located. Only the sulfur atoms of the disordered triflate anions were refined anisotropically. The diethyl ether solvent molecule is also disordered and bond length restraints were applied to facilitate reasonable modelling. The solvent molecules were refined isotropically and hydrogen atoms were not applied. One of the triflate anions was disordered over an area of diffuse electron density and a reasonable model could not be obtained despite multiple attempts including the use of rigid body constraints. The SQUEEZE (S11) function of PLATON (S12) was employed to remove the

contribution of the electron density associated with the remaining triflate and further disordered solvent molecules resulting in more satisfactory residuals. The remaining peaks of electron density (up to $1.345 \text{ e}^- \text{ \AA}^{-3}$) are all close to the disordered anions and solvent molecules, possibly indicative of some further disorder which could not be resolved.

3. Metal displacement

A (2.0 mg, 12.6 μmol , 3 equiv.), 2-pyridinecarboxaldehyde (2.4 μL , 25.3 μmol , 6 equiv.) and $\text{Cd}(\text{ClO}_4)_2$ (2.6 mg, 8.4 μmol , 2 equiv.) were mixed in CD_3CN (0.4 mL) in a J-Young NMR tube. The resulting solution was heated at 50°C for 4 hours. ^1H NMR showed the formation of cage **3a** $\cdot\text{ClO}_4$. Then $\text{Fe}(\text{ClO}_4)_2$ (2.2 mg, 8.4 μmol , 2 equiv.) was added. The atmosphere was purified via 3 cycles of evacuation/ N_2 fill and the tube was kept at 50°C overnight. ^1H NMR and ESI-MS showed clean transformation to cage **1a** $\cdot\text{ClO}_4$. ESI-MS: observed cage **1a** $\cdot\text{ClO}_4$: $[\mathbf{1a}(\text{ClO}_4)_4]^{4+}$ 659.74, $[\mathbf{1a}(\text{ClO}_4)_5]^{3+}$ 912.95.

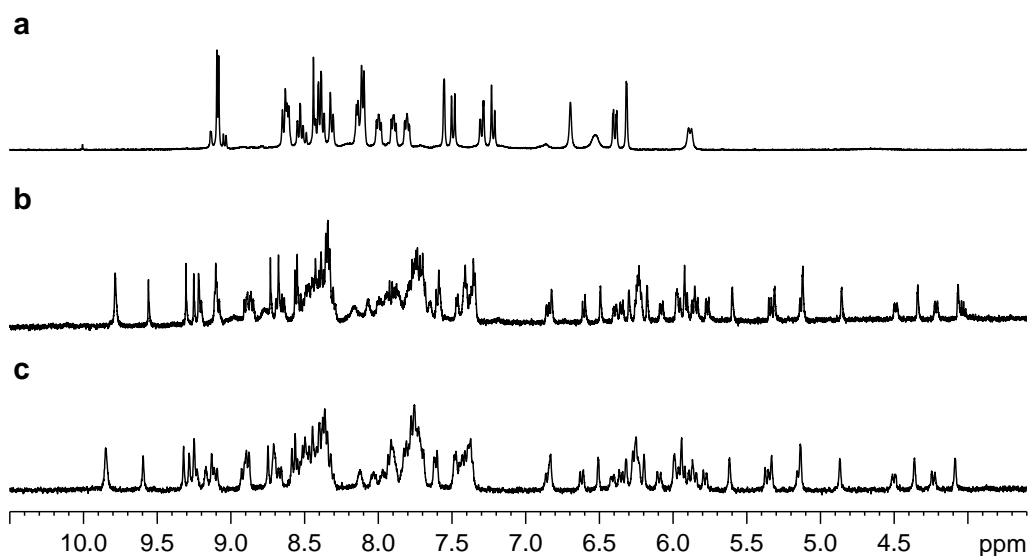


Figure S36. ^1H NMR spectra for metal displacement. **a**: reaction mixture of the formation of **3a** $\cdot\text{ClO}_4$; **b**: 50°C overnight after the addition of $\text{Fe}(\text{ClO}_4)_2$ to **a**; **c**: **1a** $\cdot\text{ClO}_4$, prepared directly from subcomponents.

4. Discussion of symmetry breaking

As shown in Fig. S37a, if the anthracenyl groups of the *anti* ligands of cage **1b** were to lie perpendicular to their actual orientation (Fig. S37c), the cage would possess an S_4 axis of symmetry joining the centroids of these anthracenyl groups. As shown in Fig. S37b, this conformation would lead to severe steric clashes between protons on neighboring anthracenyl groups, colored in orange and red. We infer, thus, that this conformation represents a higher-energy configuration than the C_1 -symmetric state observed in the solid state and by NMR in solution (Fig. S37c), in which the aromatic groups of the ligands gear together and steric clashes are minimized. The observation of NMR spectra consistent with S_4 symmetry for cages **2b** and **3a** is thus attributed to these cages' anthracenyl groups oscillating rapidly on the NMR time scale between lower-energy configurations such as the one shown in Fig. S37c through a higher-energy configuration similar to the one shown in Fig. S37b.

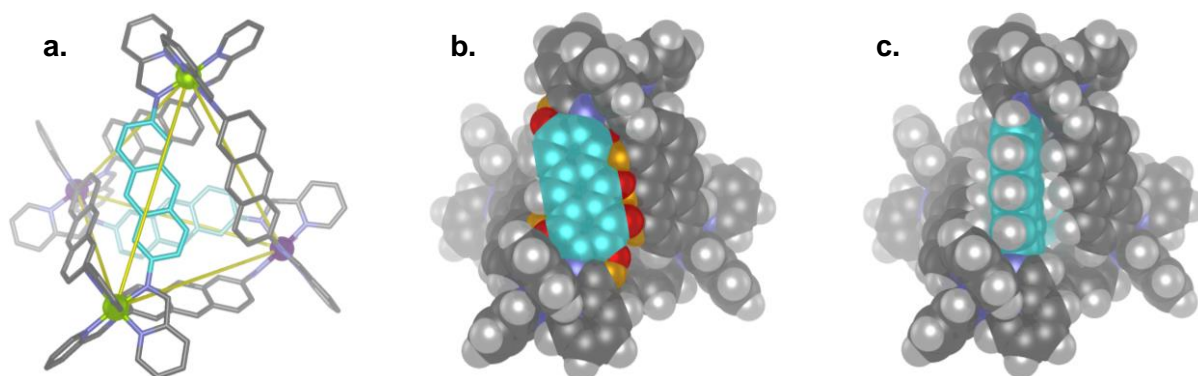


Figure S37. Comparison between a model of a hypothetical S_4 -symmetric configuration of cage **1b** and the C_1 -symmetric configuration observed in the crystal structure of **1b**. The anthracenyl groups of the *anti* ligands are colored in light blue. The two Δ and two Λ metal vertices are colored in purple and green, respectively. **a.** ball and stick presentation of S_4 -symmetric **1b**. **b.** cpk presentation of S_4 -symmetric **1b**, showing how the S_4 -symmetric state is energetically unfavorable due to steric clashes (examples of clashing atoms are colored in red and orange). **c.** CPK representation of the crystal structure of **1b**, revealing its C_1 -symmetric structure.

References

- S1. Buckman B, Nicholas JB, Serebryany V, & Seiwert SD (2011) Novel Inhibitors of Hepatitis C Virus Replication WO 2011075607 A1 20110623.
- S2. Kantam R, Holland R, Khanna BP, & Revell KD (2011) An optimized method for the synthesis of 2,6-diaminoanthracene. *Tetrahedron Lett.* 52(39):5083-5085.
- S3. Rigaku CrystalClear (Rigaku Americas and Rigaku Corporation.: 9009 TX USA 1997-2009).
- S4. CrysAlisPro (Agilent Technologies Ltd, Yarnton, Oxfordshire, UK, 2009-2011), v. 1.171.35.11.
- S5. Otwinowski Z & Minor W (1997) Processing of x-ray diffraction data collected in oscillation mode. *Methods in Enzymology* 276:307-326.
- S6. Blessing R (1995) An empirical correction for absorption anisotropy. *Acta Crystallogr.* A51(1):33-38.
- S7. Sheldrick GM (SORTAV (University of Göttingen: Germany, 1996-2008).
- S8. Farrugia L (1999) WinGX suite for small-molecule single-crystal crystallography. *J. Appl. Cryst.* 32(4):837-838.
- S9. Palatinus L & Chapuis G (2007) SUPERFLIP - a computer program for the solution of crystal structures by charge flipping in arbitrary dimensions. *J. Appl. Crystallogr.* 40(4):786-790.
- S10. Sheldrick GM (1997) SHELXL-97: Programs for Crystal Structure Analysis, University of Göttingen, Germany).
- S11. Van Der Sluis P & Spek AL (1990) BYPASS: an effective method for the refinement of crystal structures containing disordered solvent regions. *Acta Crystallogr.* A46(3):194-201.
- S12. Spek AL (2008) PLATON: A Multipurpose Crystallographic Tool (Utrecht University, Utrecht, The Netherlands).